



Dawood, A. A., Grossel, M. C., Luckhurst, G. R., Richardson, R. M., Timimi, B. A., Wells, N. J., & Yousif, Y. Z. (2017). Twist-bend nematics, liquid crystal dimers, structure–property relations. *Liquid Crystals*, 44(1), 106-126.
<https://doi.org/10.1080/02678292.2017.1290576>

Peer reviewed version

Link to published version (if available):
[10.1080/02678292.2017.1290576](https://doi.org/10.1080/02678292.2017.1290576)

[Link to publication record in Explore Bristol Research](#)
PDF-document

This is the author accepted manuscript (AAM). The final published version (version of record) is available online via Taylor & Francis at <http://www.tandfonline.com/doi/abs/10.1080/02678292.2017.1290576>. Please refer to any applicable terms of use of the publisher.

University of Bristol - Explore Bristol Research

General rights

This document is made available in accordance with publisher policies. Please cite only the published version using the reference above. Full terms of use are available:
<http://www.bristol.ac.uk/red/research-policy/pure/user-guides/ebr-terms/>

Twist-bend nematics, liquid crystal dimers, structure-property relations

Alya A. Dawood^{a,b}, Martin C. Grossel^a, Geoffrey R. Luckhurst^a, Robert M. Richardson^c, Bakir H. Timimi^a, Neil J. Wells^a and Yousif Z. Yousif^b

^aChemistry, University of Southampton, Highfield, Southampton SO17 1BJ, UK; ^bChemistry Department, Faculty of Science, Zakho University, KRG-Iraq; ^cH. H. Wills Physics Laboratory, University of Bristol, Bristol BS8 1TL, UK

Abstract

One of the current challenges in liquid crystal science is to understand the molecular factors leading to the formation of the intriguing twist-bend nematic phase (N_{TB}) and determine its properties. During our earlier hunt for the N_{TB} phase created on cooling directly from the isotropic phase and not the nematic phase we had prepared 30 symmetric liquid crystal dimers. These had odd spacers and methylene links to the two mesogenic groups; desirable but clearly not essential features for the formation of the N_{TB} . Here we report the phases that the dimers exhibit and their transition temperatures as functions of both the lengths of the spacer and the terminal chains. In addition we describe the transitional entropies, their optical textures, the X-ray scattering patterns and the 2H NMR spectra employed in characterising the phases. All of which may lead to important properties of the twist-bend nematic phase.

Graphical Abstract

KEYWORDS

Twist-bend nematics; liquid crystal dimers, local-structure correlations, N_{TB} – I transition; molecular curvature, inhomogeneity and anisotropy; orientational order

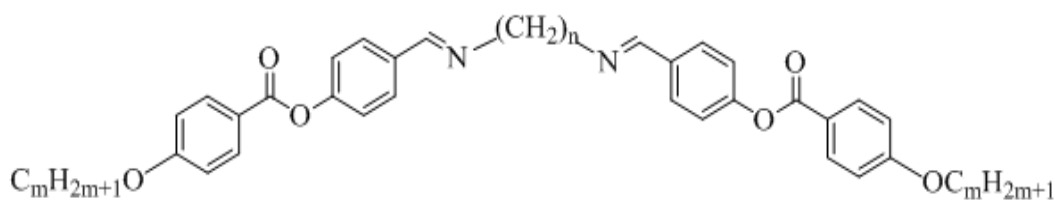
1. Introduction

The discovery of a new liquid crystal is invariably a cause for some excitement both for its discoverers and for our community. This has certainly proved to be the case for the twist-bend nematic phase, which is the fifth nematic phase to be recognised. In recent years reports of nematic-nematic transitions have aroused significant interest [1-4] and this certainly grew when it was realised that for some the low-temperature nematic phase was the twist-bend nematic phase predicted by Meyer [5] and then, much later, by Dozov [6]. The organisation of the director in the phase has a helicoidal structure that is analogous to the chiral nematic phase but with the director tilted with respect to the helix axis. The pitch of the helix has been shown to be strikingly small [7-9], of the order of 8nm as anticipated by Dozov. It has been shown that the constituent molecules do not need to be chiral for the helix to form. According to Dozov what is required is that the twist elastic constant, K_3 , should **CONTACT** Geoffrey R. Luckhurst G.R.Luckhurst@soton.ac.uk

decrease with decreasing temperature and pass through zero at which point the nematic would transform to the N_{TB} phase. In his seminal paper he suggested that this behaviour of K_3 is to be expected for a bent-core molecule. Indeed the predicted phase behaviour has been observed by Chen *et al.* [10] for UD68, a semi-rigid bent-core mesogen and by Wang *et al.* [11] for a more flexible bent-core system.

Prior to this observation a liquid crystal dimer with a flexible spacer having an odd number of methylene groups attached directly to two cyanobiphenyl groups namely 1'',7''-bis(4'-cyanobiphenyl-4-yl) heptane (CB7CB) was also shown by Cestari *et al.* [12] to form the N_{TB} phase. In the all-trans structure of this dimer the molecule does have the curvature that might be expected to form the twist-bend nematic phase. However, as we shall see in Appendix A, the definition of the curvature or bend of such a mesogenic molecule is not straightforward. At a macroscopic level the bend elastic constant for CB7CB is predicted by molecular field calculations which include the spacer flexibility to be small and to decrease with increasing orientational order as required for the formation of the N_{TB} phase [12]. Before and even after this assignment other dimers with odd spacers and methylene links had been shown to exhibit nematic-nematic transitions [2-4, 13]; although the low-temperature nematic phase had not been identified for these it now seems clear that it is the N_{TB} phase. Subsequently there have been many studies which have reported the formation of the twist-bend nematic phase by odd liquid crystal dimers with most having methylene links to the mesogenic groups [12,14, 15-17]. However, a few dimers with other links, for example ether, can also be persuaded to form the N_{TB} phase, enantiotropic, monotropic or virtual [19-21]. This difference in behaviour between ether- and methylene-linked odd dimers is consistent with differing topology at the link as found by rather basic molecular field calculations.

For the vast majority of such systems the twist-bend nematic phase is formed on cooling the nematic phase. But the analogy between the smectic A and the N_{TB} phase [22, 23] as well as an extended Maier-Saupe theory [24] suggests that it should also be possible to form this phase directly from the isotropic phase. If so it would open up new challenges to theory to explain the transition as well as opportunities to characterise the new nematic phase under quite novel conditions. In fact the N_{TB} – I transition has been observed for a methylene linked nonane dimer when a chiral dopant is added to it [25]. An alternative strategy is to modify the structure of a symmetric dimer by varying the lengths of the odd spacer and the terminal chain. This was adopted for the N,N''-bis[4'-(4''-alkyloxybenzoyloxy)benzylidene]alkane- α,β -diamines [2] -with the structure



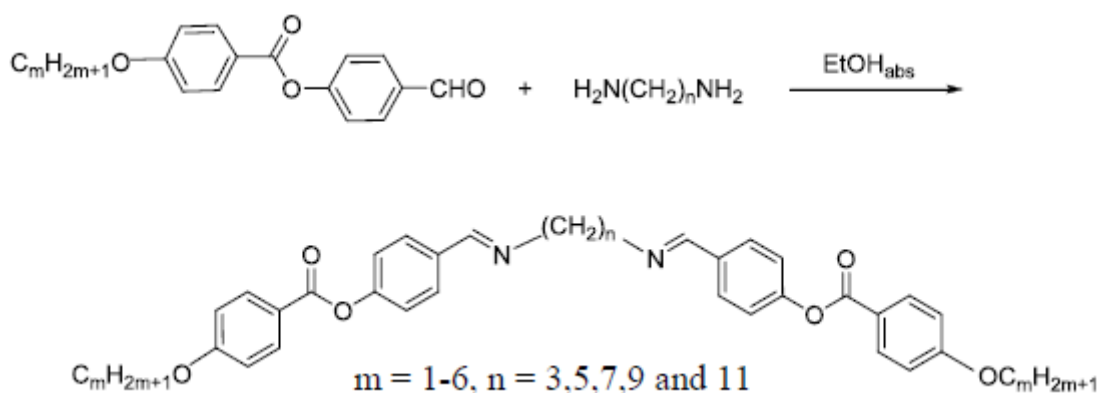
and denoted by the mnemonic *mO.n.Om* [26]. To determine the optimal values of the spacer, *n*, and the terminal chain, *m*, we had synthesised 30 dimers where *n* adopted odd values from 3-11 and *m* was given values 1-6. Of these the dimer 2O.3.O2 was found to form the twist-bend nematic directly from the isotropic phase. Here we take the opportunity to report the synthesis, characterisation and some properties of the dimers that we have not published previously. Our reasons for making this significant body of data on these liquid crystal dimers available is to enhance further understanding of how the dimers' structure can influence the phases, particularly the twist-bend phase, as well as to determine certain of its properties as others have done.

The organisation of our paper is as follows. In the next section we describe in outline the generic synthesis of the dimers together with the techniques used to characterise them, their phases and phase transitions. In Section 3 we give a selection of our experimental results and discuss our understanding of them. Section 4 describes our investigations based on X-ray scattering and ^2H NMR spectroscopy. Our conclusions are in Section 5.

2. Experimental

2.1 Preparation

The synthesis of the dimers *mO.n.Om* has been described. The reaction pathway is outlined in Scheme 1. The reagents were purchased from Aldrich, UK and the benzoate esters were prepared following the route reported by Thacker *et al.* [27]. The Schiff base dimers can be subject to decomposition and so were prepared under dry nitrogen. In addition their experimental studies were also performed under dry nitrogen. The products were purified by crystallisation twice from dry ethanol. The resultant white powders were dried *in vacuo*. These were characterised by NMR spectroscopy both ^1H and ^{13}C , electrospray mass spectrometry and IR spectroscopy. Elemental analysis was employed to confirm the purity of the liquid crystal dimers. Exemplar data for a selection of the dimers is shown as Supplemental [Information](#).



Scheme 1. The synthetic pathway to the liquid crystal dimers *mO.n.Om*.

2.2 Mesophase investigation

The properties of the dimers investigated were (a) the transitional enthalpy and associated transition temperature, (b) the optical texture, (c) the X-ray scattering pattern and (d) the ^2H NMR spectrum. The latter three properties were studied as a function of temperature. The equipment used in these experiments was (a) DSC: Universal V4.5A TA model DSC Q1000. (b) Optical microscopy: Zeiss polarising microscope equipped with a Linkam TP 94 hotstage and temperature controller. (c) X-ray: Ganesha 300 XL apparatus; Genix 3D source with copper $K\alpha$ radiation and a Pilatus 300k detector. The sample and detector were kept in vacuo. It was also aligned with a magnetic field of up to 1T. A Eurotherm 818 P controller was connected to a bespoke heater. (d) NMR: 400 MHz Bruker AVII spectrometer using a single pulse sequence with a 9.40T magnetic field. The sample temperature was calibrated using the ^1H NMR spectrum of ethylene glycol dissolved in DMSO-d_6 .

3. Results and discussion

3.1 Transitional properties and phases

We shall start with the transitional properties of the liquid crystal dimers that we have synthesised. Their phases have been identified primarily from their optical textures and mobilities as judged by the Brownian-like director fluctuations. This identification has been supported by the transitional entropies which are related to the properties of the phases involved, their ^2H NMR spectra which provide a powerful indication of the phase chirality and the X-ray scattering pattern. The process we have adopted will become clear as we discuss the results for the properties of the liquid crystal dimers. The most complete description of our investigation of the $mO.n.Om$ is contained in the Doctoral Thesis of Dr. A. A. Dawood [28], here we shall focus of the major aspects of this.

It is sensible to describe and discuss how the transitional properties of the odd dimers $mO.n.Om$ change along homologous series formed by varying the spacer length while keeping the terminal chain length constant and also by varying the terminal chain length while keeping the spacer length constant. Here the odd spacer is found to play a significant role in stabilising the twist-bend nematic phase as well as determining its properties which relate to the molecular curvature. This contrasts with the transitional behaviour of dimers where the spacer length is kept constant and the length of the terminal chain is varied. As this increases other phases are inserted and the formation of the twist-bend nematic can be blocked. The primary data for the phase identities, transition temperatures, enthalpies and entropies, as determined by DSC, are listed in Tables 1-5; we note that some of these dimers have been synthesised previously and they are identified with the references in the Tables.

3.1.1 Dimers $1O.n.O1$

In the first comparison of the transitional properties we plot, in Figure 1(a), the transition temperatures as a function of the spacer length, n , for the dimers $1O.n.O1$ with their methoxy terminal groups. What is apparent and of real interest is that the dimer with the shortest spacer, $1O.3.O1$, does form the N_{TB} phase, albeit monotropic, directly from the isotropic phase. The optical texture for the N_{TB} phase supercooled to 30°C which is about 30°C below $T_{N_{TB}I}$ is shown in Figure 2 and has the polygonal form often found for this phase. The scaled transitional entropy, $\Delta S_{N_{TB}I}/R$, for the first-order $N_{TB} - I$ transition is shown in Figure 1(b) together with other members of this series. It is clear that the entropy change is very large at 0.68 in comparison to those for the $N_{TB}-N$ transition which are about 0.1 in keeping with that expected for a $N_{TB} - I$ transition and found for the related dimer $2O.3.O2$ [26]; there are some slight differences in behaviour and we shall return to these shortly. Such behaviour is in keeping with that found for $SmA-I$ and $SmA-N$ transitions [29], again supporting the analogy proposed between the SmA and N_{TB} phases [22,23].

Figures for $mO.n.Om$ Dimers

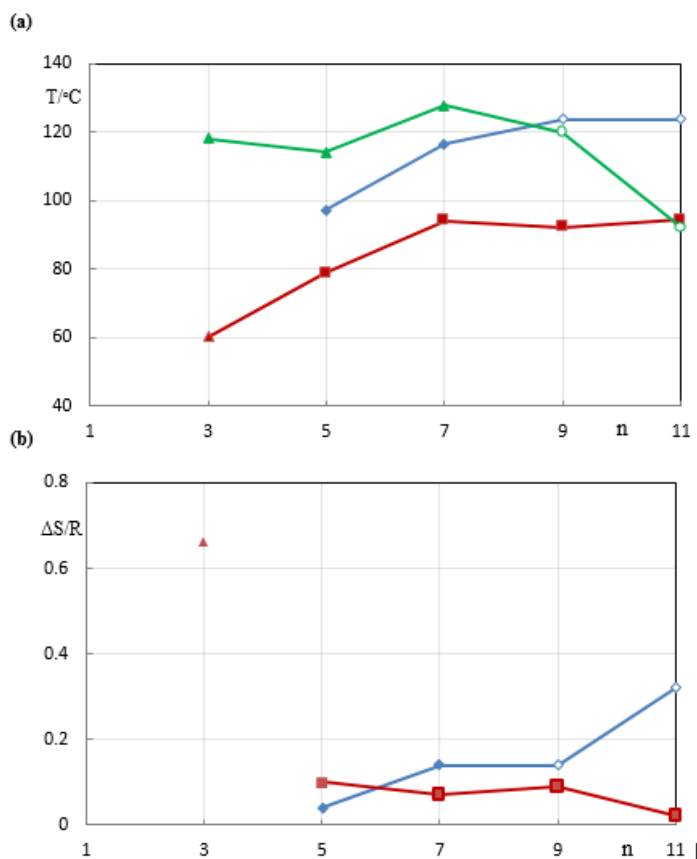


Figure 1. (colour online) Dimers $1O.n.O1$ (a) The dependence of the transition temperatures, T , on the length of the alkane spacer, n and (b) the dependence of the scaled transitional entropies, $\Delta S/R$, also on n . The symbols used to denote the temperatures and transitional entropies are \blacktriangle for $Cr - I$; \circ for $Cr - N$; \blacktriangle for $(N_{TB} - I)$; \blacksquare for $(N_{TB} - N)$; \circ for $N - I$; \diamond for $(N - I)$. Here () denotes a monotropic transition.



Figure 2. (colour online) The optical texture for the N_{TB} phase of 10.3.O1 at 30°C supercooled from the isotropic phase. The sample was contained between thin and untreated glass slides.

The availability of the results for the N_{TB} -N transition for higher homologues allows us to speculate on the origin of the N_{TB} – I transition for the dimer 10.3.O1. This might be expected if on passing from 10.5.O1 to 10.3.O1 T_{NI} decreased with respect to $T_{N_{TB}N}$ or the reverse that is $T_{N_{TB}N}$ increased with respect to T_{NI} . From the results for 10.5.O1 and 10.7.O1 we could extrapolate to the dimer with n equal to 3. However, the lines for T_{NI} and $T_{N_{TB}N}$ do not intersect so that, based on the existing data, it could be concluded that the N_{TB} -I transition should not exist for 10.3.O1. It is possible to progress if we have a dimer series which included one with a spacer length of 3 existed. This is the case for a series of cyanobiphenyl dimers with an ether-linked spacer $CB.O(n-2)O.CB$ where the two oxygen links form part of the spacer and this has been well studied [30,31]. The dependence of T_{NI} on the odd spacer lengths from 3 to 11 is shown in Figure 3(a) and it seems that the decrease in T_{NI} between dimers with n of 5 and 7 are similar to those for 10.5.O1 and 10.7.O1. However, it is immediately apparent that T_{NI} for CBO.1.OCB drops dramatically to that for CBO.3.OCB unlike those for other members of the series. It would appear, therefore, that from the evidence currently available the direct transition from the isotropic to the twist-bend nematic phase occurs for the dimer 10.3.O1 occurs because the N-I transition temperature drops more rapidly than that for the N_{TB} -N transition.

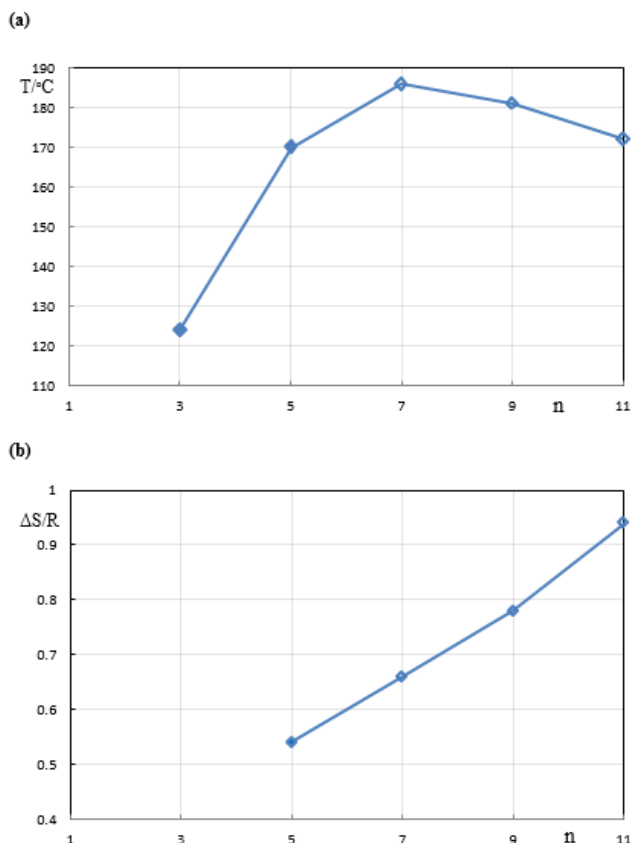


Figure 3. The variation of (a) the nematic-isotropic transition temperature, T , and (b) the associated transitional entropy, $\Delta S/R$, for the ether-linked cyanobiphenyl dimers CB.O($n-2$).CB where n is the number of atoms in the spacer including the two oxygen atoms. The two dimers, with n of 3 and 5, exhibit monotropic transitions. The symbols used to denote transition temperatures are: ♦ for (N-I) and ♦ for N-I. Here (♦) denotes a monotropic transition.

It is also of interest that, along the homologous series of the odd dimers, 1O. n .O1, T_{NI} increases with n but to a decreasing extent, indeed those for n equal to 9 and 11 are essentially the same. At least qualitatively this variation of T_{NI} with n could result from an increase in the molecular anisotropy or a decrease in the molecular biaxiality. At a more quantitative level any theory aiming to explain such behaviour must include the flexibility of the spacer and the molecular anisotropy of each conformer. Indeed such theories have been developed to account for the dramatic odd-even effects along homologous series such as CB.O($n-2$).O.CB [31]. For some theories the conformational states of the spacer have been described with the Flory rotational isomeric state model in which the alkane spacer can adopt combinations of t, g^+ and g^- configurations [32]. This model was found to work reasonably well in accounting for the properties of the early members, both odd and even, of the CB.O($n-2$).O.CB series. However, for the later members the alternation in the properties - T_{NI} and $\Delta S_{\text{NI}}/R$ - predicted is found not to attenuate as fast as that found experimentally. In order to predict the attenuation in the properties more realistically, especially for longer spacers for $n \sim 18$, it is necessary to employ a continuous description of the conformational states by using a torsional potential such as that developed by Ryckaert and Bellemans [33]. However in the context of the twist-bend nematic problem where the spacers are odd it is of relevance to note that the predictions

of T_{NI} and $\Delta S_{NI}/R$ for such homologous series are similar for both torsional potentials, discrete and continuous [34]. They are all also in reasonable agreement with experiment for the CB.O($n-2$).O.CB dimers. It is unlikely that calculations based on just a single all-trans conformer would provide the same agreement.

We can now consider the results of primary interest namely how the transition temperatures, T_{NtbN} , and transitional entropies, $\Delta S_{N_{TB}N}/R$, vary with the spacer length given the background provided by the N-I transition. What is apparent from Figure 1(a) is that $T_{N_{TB}N}$ begins by increasing with increasing n but that for the last three members of the series the transition temperature is essentially constant. Interestingly the growth in T_{NtbN} might be taken to show that the molecular curvature increases as the spacer length increases but what we do not know is how the molecular anisotropy, which certainly influences T_{NI} , also contributes to $T_{N_{TB}N}$. The issue is that we have contributions of molecular anisotropy and curvature to both transition temperatures. For the N-I transition an increase in the anisotropy would be enhanced by a decrease in the curvature both increasing T_{NI} but an increase in the curvature might be expected to reduce the influence of the molecular anisotropy. For $T_{N_{TB}N}$ an increase in both the anisotropy and the curvature with spacer length would be expected to increase the transition temperature. What we find is that T_{NtbN} reaches a plateau suggesting that the influence of the anisotropy and this poses us with a problem waiting to be resolved. The transitional entropies may provide some insight into the problem and these are shown for the 1O. n .O1 homologous series in Figure 1(b). What this shows is that $\Delta S_{NI}/R$ clearly grows with the spacer length, n , in keeping with that found for the CB.O($n-2$).O.CB series and shown in Figure 3(b) the difference being that the magnitude in $\Delta S_{NI}/R$ is significantly larger than for the 1O. n .O1 dimers in accord with their greater biaxiality compared with the ether linked dimers. **This difference in the behaviour of the transitional entropy for liquid crystal dimers has also been observed experimentally by Henderson *et al.* [35] and is in keeping with earlier molecular-field based predictions [36].** The entropy change at the N_{TB} -N transition is plotted in Figure 1(b) against the spacer length apart from the relatively small value of $\Delta S_{N_{TB}N}/R$ it indicates that the transition entropy decreases with increasing n which suggests that the molecular curvature grows with the spacer length. As we have seen there are two reliable molecular field theories which can be employed to predict the properties at the N-I transition. This is not the situation for the N_{TB} -N transition, indeed the extended Maier-Saupe theory [9] predicts this transition to be continuous whereas experiment and the symmetries of the two phases shows that the transition should be first order [37].

3.1.2 Dimers 3O. n .O3

The results for the homologous series 2O. n .O2 have already been published [26] and so here we give those for the dimers with two propoxy terminal groups. The results are shown in Figure 4(a). A striking feature is that it did not prove possible to observe a transition to either a twist-bend nematic or a nematic phase for the second

dimer of the series. This was despite numerous attempts to supercool the isotropic phase; presumably its melting point is just too high. However, we were able to determine the virtual $T_{N_{TB}I}$ for the first, as described in Section 3.1.5. It was possible to supercool that for the next member 3O.7.O3 and thus observe the monotropic N and N_{TB} phases. Both of these phases are also found for the higher homologue 3O.9.O3; the nematic transition is enantiotropic. For the last member of the series with an undecane spacer an enantiotropic nematic phase is seen but not the twist-bend nematic phase, again despite many attempts to trap it. The variation of the few values of T_{NI} and $T_{N_{TB}N}$ with n determined are found to be consistent with those seen for the methoxy dimers. Thus T_{NI} increases from $n = 7$ to 9 and then is constant. Similarly $T_{N_{TB}I}$ increases slightly from $n=7$ to 9 compared to the small decrease for the small decrease found for the methoxy dimers. There is a more significant difference namely that the transition temperatures for the propoxy dimers are about 10°C lower than those for the corresponding methoxy dimers and we shall return to this in Section 3.1.5.

The variation of the transitional entropy with the spacer length, shown in Figure 4(b), is more striking. Thus $\Delta S/R$ for the N-I transition increases with the spacer length in accord with the growth of the orientational order. For the N_{TB} – N transition the entropy change decreases slightly with increasing n suggesting a decrease in the order or an increase of curvature with decreasing spacer length.

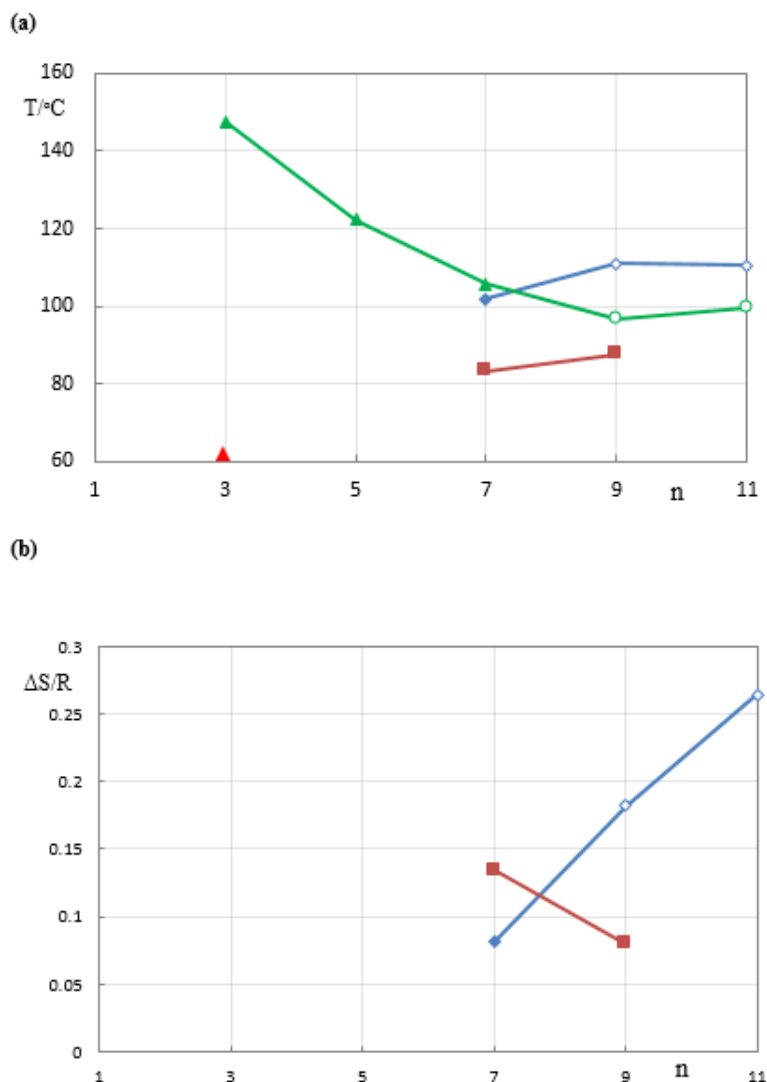


Figure 4. (colour online) Dimers 3O.n.O3 (a) The dependence of the transition temperatures, T_i , on the length of the alkane spacer, n and (b) the dependence of the scaled transitional entropies, $\Delta S/R$, also on n . The symbols used to denote the temperatures and transitional entropies are \blacktriangle for Cr – I; \circ for Cr – N; \blacktriangle for (N_{TB} – I); \blacksquare for (N_{TB} – N); \diamond for N – I; \blacklozenge for (N – I). Here () denotes a monotropic transition.

3.1.3 Dimers 4O.n.O4

The transition temperatures for this series of dimers are shown in Figure 5(a) and unlike the previous series all members do exhibit mesophases both enantiotropic and monotropic. One particularly interesting feature is that the first three dimers, 4O.3.O4, 4O.5.O4 and 4O.7.O4, exhibit a B₆ following an isotropic, nematic and twist-bend nematic phase, respectively. The B₆ phase, normally found for bent-core mesogens, is a disordered lamellar phase with an intercalated structure which in a sense resembles an intercalated smectic C phase [38, 39]. The identification of the B₆ phase for dimers with pentane and heptane spacers was made by Šepelj *et al.* [2], they

showed that the dimer 8O.7.O8 was totally miscible with the bent-core mesogen **1S** based on 1,3-diaminobenzene which exhibits a B₆-I transition [40]. In addition contact preparations between 8O.7.O8 and other dimers in the two series, *m*O.5.O*m* and *m*O.7.O*m*, where *m* extended from 4-12 revealed the prevalence of the B₆. Our own studies using analogous techniques revealed the existence of the B₆ phase for the other odd spacer lengths including the optical texture such as that given in Figure 6 for 4O.3.O4; this shows the jagged bâtonnets formed from the isotropic phase prior to the appearance of the phase with its natural focal conic texture. In addition the dimers 4O.5.O4 and 4.7.O4 have also been shown [2] to exhibit the B₆ phase, again monotropic, although the first also exhibits the monotropic N phase while the second forms both the enantiotropic N and monotropic N_{TB} phases. The very strong entropy change at the B₆ – I transition shown in Figure 5(b) by the 4O.3.O4 dimer is also with this assignment.

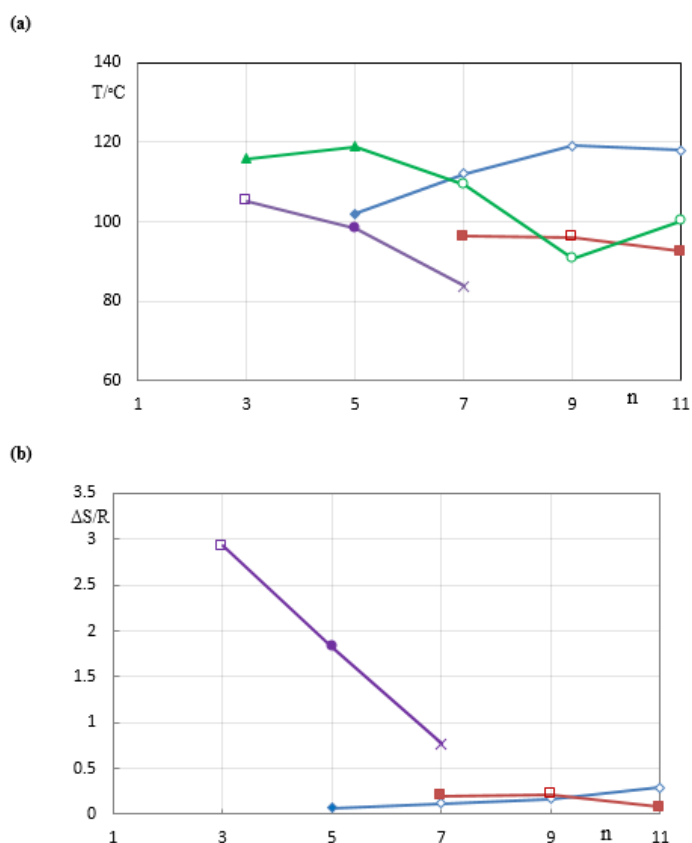


Figure 5. (colour online) Dimers 4O.*n*.O4 (a) The dependence of the transition temperatures, T , on the length of the alkane spacer, n and (b) the dependence of the scaled transitional entropies, $\Delta S/R$, also on n . The symbols used to denote the temperatures and transitional entropies are \blacktriangle for Cr – I; \circ for Cr – N; \square for (B₆ – I); \bullet for (B₆ – N); \times for (B₆ – N_{TB}); \square for N_{TB} – N; \bullet for \emptyset ; \diamond for N – I; \blacklozenge for (N – I). Here \emptyset denotes a monotropic transition.

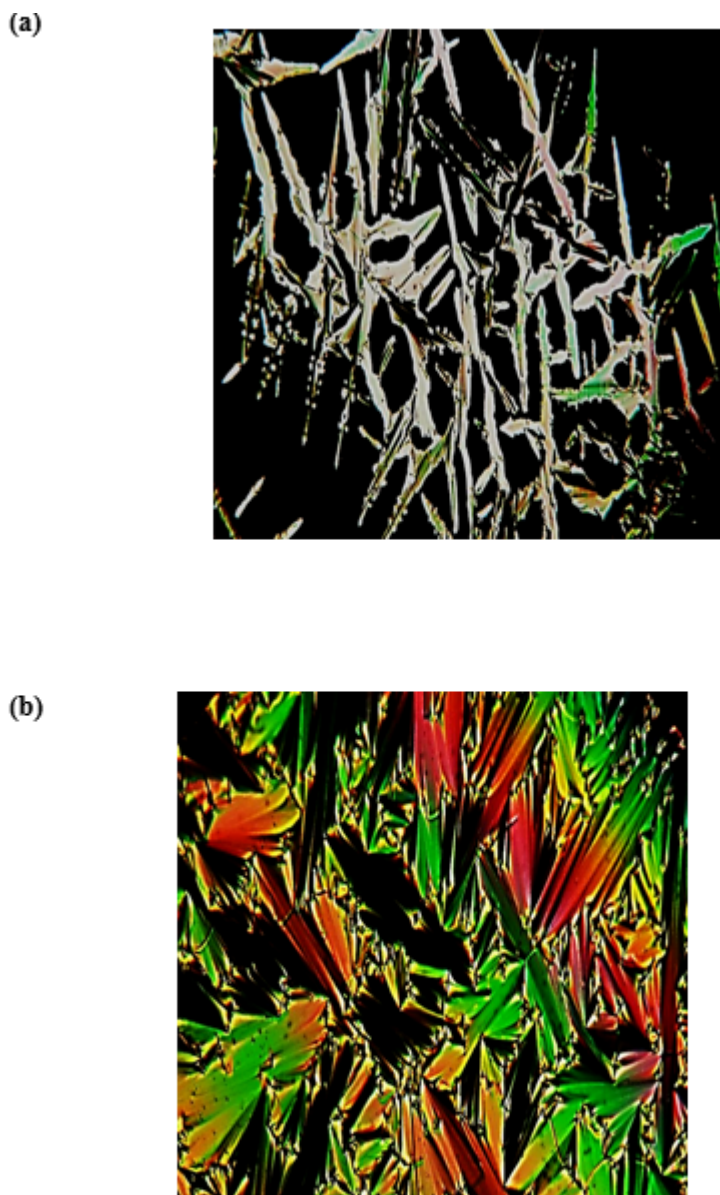


Figure 6. (colour online) The optical textures for the dimer 4O.3.O4 for (a) the **jagged** bâtonnet in the biphasic region at 105°C prior to the B₆ phase and (b) the fan-like texture at 102°C.

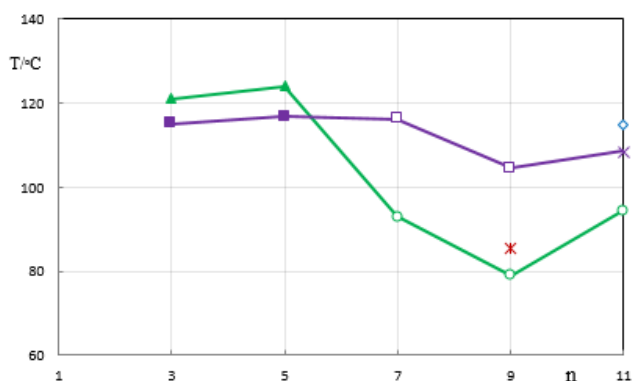
It is of interest to consider the variation of the transition temperatures shown in Figure 5(a) with the spacer length. This variation shows that the lamellar structure is formed provided the terminal chain is long in comparison to the spacer length. These and the results we shall see later indicates that provided the terminal chain is longer than about half the spacer length then it seems that the molecular homogeneity is sufficient to stabilise the layered structure of the B₆ phase. This behaviour is analogous in part with that found for the symmetric dimers α,ω -bis(4-*n*-alkylanilinebenzylidene-4'-oxy)alkanes [41]. However for these systems an intercalated phase was not formed as it is for the *mO.n.Om* dimers. As with the earlier series T_{NI} increases although slightly with *n*. In contrast $T_{N_{TB}N}$ tends to decrease but very slightly for *n* equal to 7, 9, and 11 more or less as found for the 1O.*n*.O1 dimers. The

three transitions to the B₆ phase show a clear decrease with n partly associated with the weakening of the inequality $m > n/2$ but in addition it should be recalled that the transitions involve different phases I, N and N_{TB} so that it is hard to quantitative conclusions. The entropy changes $\Delta S/R$ for the N-I transition grows with n as found earlier. That for the N_{TB} – N transition tends to decrease with increasing n which is in accord with the later members of the previous series. Strictly there are not strictly comparable transitions involving the B₆ phase, however the large entropy change is found to decrease, but this could be associated with the fact that the associated phases are I, N and N_{TB}.

3.1.4 Dimers 6O.n.O6

The results for the longest terminal chain where $m = 6$ are shown in Figure 7; these certainly surprised us because the series was dominated by the B₆ phase with the first two members being monotropic. In addition there was a solitary monotropic 'B₆ phase, an enantiotropic N phase as well as the enantiotropic B₆ phase. The first three T_{B6I} are essentially independent of the spacer length; there is then a small decrease to the nonane dimer and for the undecane dimer the B₆ is formed from the nematic phase. Thus although there is a large variation in the spacer length along the homologous series these transition temperatures do not change significantly. Presumably the reason for this is that the driving force for the creation of the B₆ phase is related to the terminal chain together with the bent shape of the odd dimers which is reflected by the intercalated structure of the phase. However, the variation of the bent shape along the series strangely does not seem to influence the structure of the phase. It is also of interest that the transitional entropy shown in Figure 7(b) varies with the spacer length by only a relatively small amount, although at the end of the series there is a small drop which results from the transition being from N to B₆ rather than from I. The entropy change for the N-I transition is perhaps slightly larger than for the other terminal chains but the difference is not significant. Finally we note that the entropy change for 'B₆ – B₆ seems weak in keeping with other measurements.

(a)



(b)

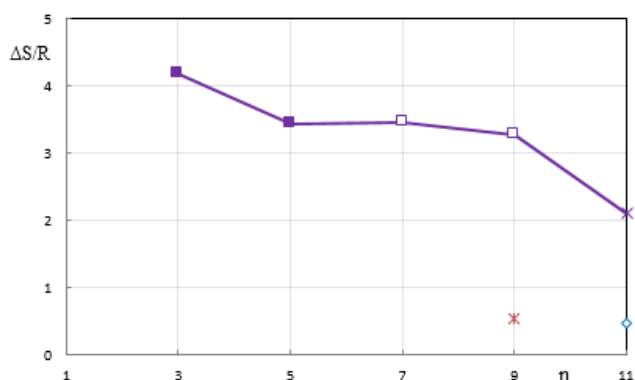


Figure 7 (colour online) Dimers 6O.*n*.O6 (a) The dependence of the transition temperatures, T_i , on the length of the alkane spacer, n and (b) the dependence of the scaled transitional entropies, $\Delta S/R$, also on n . The symbols used to denote the temperatures and transitional entropies are \blacktriangle for Cr - I; \circ for Cr - B₆ or, for $n=9$, B₆ - Cr; \blacksquare for (B₆ - I); \square for B₆ - I; \times for (B₆ - B₆); \times for B₆ - N; \diamond for N - I. Here () denotes a monotropic transition.

3.1.5 Dimers mO.3.Om

In the previous four sections we have explored how the transitional properties of the liquid crystal dimers vary with the length of the odd spacer, and implicitly the bend, which in many ways may be thought of as their primary structural feature. It is, however, of some interest to see how the properties change with the terminal substituent, in this case the length of the alkyl chain takes odd and even values; now the length of the odd spacer is kept fixed. Three series will be considered in which n is assigned values of 3, 7 and 11.

We shall start with the homologous series mO.3.Om. The results for the transition temperatures are shown in Figure 8(a) and these are somewhat sparse with each dimer exhibiting a single mesophase. Half of these are the N_{TB} phase and the other half the B₆ phase. The N_{TB} phases are formed directly from the isotropic phase with the transition temperature of 1O.3.O1 being lower than that for the next homologue of the series. The homologue 3O.3.O3 has a lower $T_{N_{TB}I}$ comparable to that of 1O.3.O1 but because the melting point is so high it proved extremely difficult to supercool the compound to observe this N_{TB} phase. We did manage to obtain this

sporadically but were able to confirm the results by using a mixture of 3O.3.O3 with 2O.5.O2 which forms monotropic N and N_{TB} phases. The equimolar mixture forms just a N_{TB} phase at about 78°C and this gives a virtual transitional temperature of about 62°C; a similar extrapolation was used to confirm the transition temperature for 2O.3.O2 [26]. This is still a rare transition but one which offers new opportunities to help with understanding aspects of the twist-bend nematic phase under special conditions. We shall defer a discussion of the variation of the $T_{N_{TB}I}$ until the next series which has a richer phase behaviour. At the other end of the series there are three B₆ phases which are also monotropic and formed directly from the isotropic phase. They have very similar transition temperatures which, as for smectics, may be related to the molecular inhomogeneity in driving the formation of this lamellar structure. The tentative rule that we had introduced in Section 3.1.3 governing the stability of the B₆ phase, namely $m > n/2$, seems not to apply here in since 3O.3.O3 and 2O.3.O2 do not exhibit the B₆ phase. Perhaps their formation of the N_{TB} phase instead results from the shorter spacer for these dimers. The variation of the entropy changes for the N_{TB}-I and the B₆-I transitions with the terminal chain length are shown in Figure 8(b) although we were not able to determine that for 3O.3.O3. As we have seen, the values for these twist-bend nematic-isotropic transitions are large in comparison with the values found for the N_{TB}-N transitions, a result in keeping with the analogy between the behaviour of the smectic A and N_{TB} phases [22,29]. However the scaled entropies, $\Delta S/R$, are small in comparison with those for the B₆ which also show an increase from about 3 to 4 as the terminal chain length, m , grows and for 4 to 6 is perhaps associated with an increase of the order of the phase.

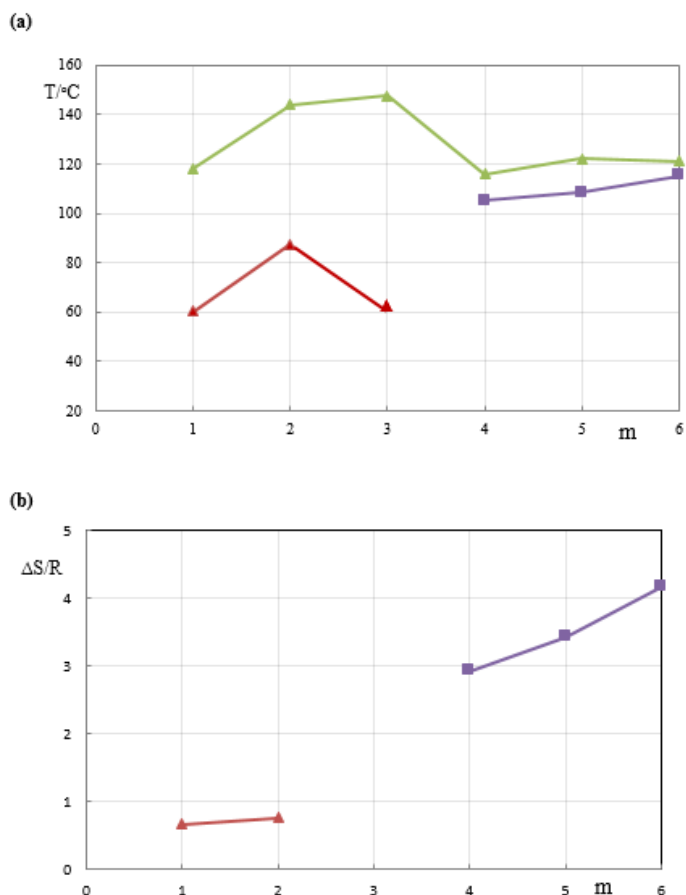


Figure 8 (colour online) The dependence of (a) the transition temperatures, T , and (b) the scaled transitional entropies, $\Delta S/R$, on the number of carbon atoms in the terminal alkyloxy chains for the dimers $m\text{O}.3.\text{Om}$. The symbols used to denote the transition temperatures and transitional entropies are \blacktriangle for Cr-I, \blacksquare for ($\text{B}_6\text{-I}$) and \blacktriangle for ($\text{N}_{\text{TB}}\text{-I}$). () denotes monotropic transitions.

3.1.6 Dimers $m\text{O}.7.\text{Om}$

The variations of the phases and transition temperatures with the length of the terminal chain are shown in Figure 9(a); they have a particular curiosity. Five of the transitions are monotropic but, with the exception of just, $\text{B}_6\text{-N}_{\text{TB}}$, exhibited annoyingly by $4\text{O}.7.\text{O}4$, we were able to work with these. One feature that stands out is the clear odd-even effect and its attenuation shown by the N-I transition. In fact this effect is well-known for monomers, such as the 4-alkyloxy-4'-cyanobiphenyls [42]. This odd-even behaviour for monomers can be understood in terms of a molecular field theory which includes the flexibility of the chain [43] although here a simple interpretation will be sufficient. The terminal chain in a cyanobiphenyl monomer is shown schematically in Figure 10 for three chain lengths, 1, 2 and 3 attached by O to the mesogenic core. What is clear is that, for the first, the methyl group is aligned at an angle to the para axis of the mesogenic group. For the second member the methyl group is now parallel to the para-axis thus increasing the molecular anisotropy so that this is larger than for a single methyl group. For the third member the methyl group is tilted with respect to the para-axis which reduces

the molecular anisotropy; although the molecular biaxiality also changes. At this level we would expect the N-I transitions would decrease from 1 to 2 and then from 2 to 3. The same simple argument would also apply to dimers; indeed it has long been realised that the general effect of terminal groups in monomers also applies to dimers [44]. However what is not perhaps so well-known is that changes in the N-I transition temperatures for dimers are also reflected in the N_{TB} -N transition temperatures as is clearly apparent for the dimers *mO.7.Om* in Figure 9(a). This parallel behaviour suggests that the N_{TB} -N transition is, like the N-I transition, related to the anisotropy of the mesogenic groups of the dimer at least when the spacer linking them is the same. There are three B_6 phases for the last members of the series which exhibit a B_6 - N_{TB} and two B_6 -I transitions. The dimers 4O.7.O4 and 6O.7.O6 have been shown by Šepelj *et al.* [2] to form the B_6 phase and so it would seem reasonable that the dimer 5O.7.O5 which we have studied should also form a B_6 phase. We have, however, been able to confirm this by studying the miscibility of 4O.7.O4 with 5O.7.O5. The phase diagram is shown in Figure 11 where the transition temperatures are given as a function of the mole fraction of 5O.7.O5. As the dimer 5O.7.O5 is added to 4O.7.O4, with its phase sequence $B_6 - N_{TB} - N - I$, so T_{NI} decreases relatively slowly over essentially the entire composition range, as expected $T_{N_{TB}N}$ also decreases but over a much smaller concentration range, In contrast $T_{B_6N_{TB}}$ grows more rapidly, again over the entire composition range passing through the $N_{TB} - N$ and $N - I$ phase boundaries and reaching the $B_6 - I$ transition for essentially pure 5O.7.O5. Thus providing a confirmation that the phase formed by the dimer 5O.7.O5 is indeed a B_6 . Here, unlike the series *mO.3.Om*, the increase in the transition temperature to the B_6 phase is in keeping with the rule which requires $m > n/2$ and is presumably related to the growth in the molecular.

The entropy changes along the series shown in Figure 9(b) for the N-I transitions are small and there is no indication of a systematic variation with the length of the terminal chain. In contrast for the N_{TB} -N transition there is a systematic growth in the entropy change which is relatively hard to rationalise related as it is to the order of both phases. The entropy changes for the transitions involving the B_6 phase are given in Figure 9(b) and as expected the results for the B_6 -I transition are striking for their magnitude, 2.63 and 3.45. However, for the B_6 - N_{TB} transition the entropy change is just 0.84 which presumably results from the higher orientational order of the N_{TB} phase.

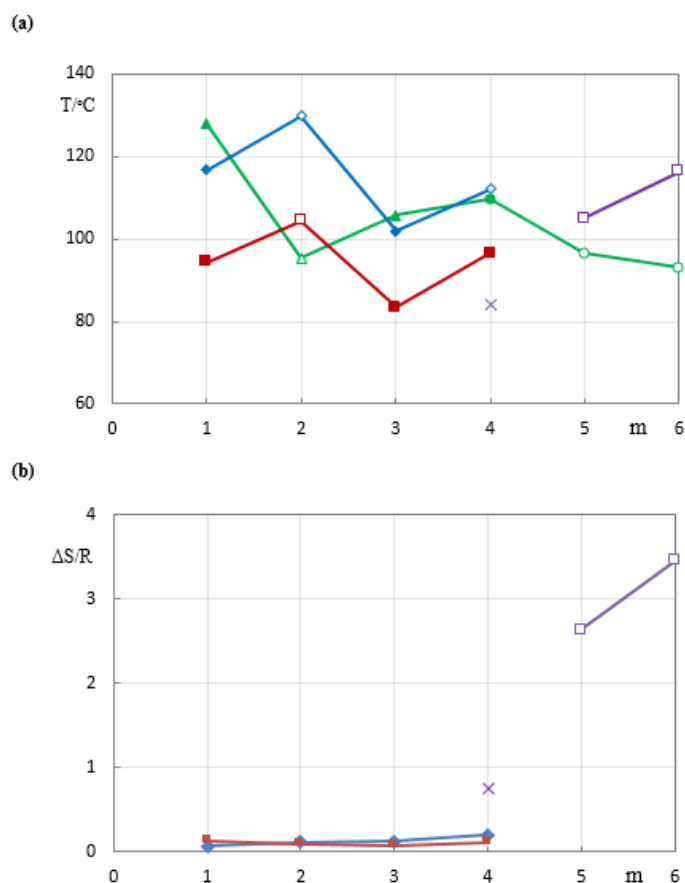


Figure 9. (colour online) The dependence of (a) the transition temperatures, T , and (b) the scaled transitional entropies, $\Delta S/R$, on the number of carbon atoms, m , in the terminal alkyloxy chains for the dimers, $mO.7.Om$. The symbols used to denote the transition temperatures and transitional entropies are \blacktriangle for Cr-I; \blacklozenge for Cr - NTB; \circ for Cr - B₆; \bullet for C-N; \square for B₆ - I; \blacksquare for NTB - N; \square for (NTB - I); \times for (B₆ - NTB); \diamond for N - I; \blacklozenge for (N - I). () denotes monotropic transitions.

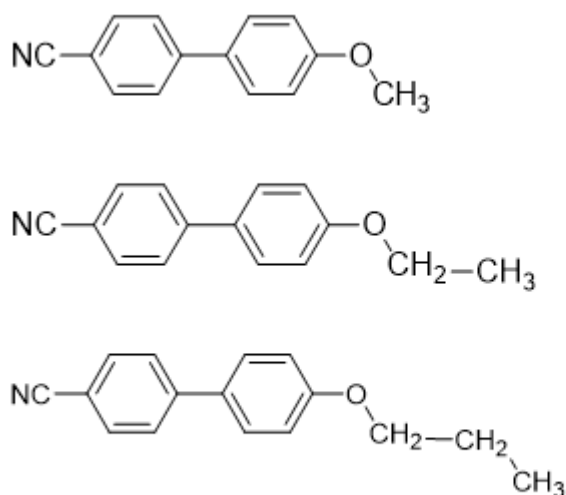


Figure 10. A sketch of the molecular structure of cyanobiphenyl monomers with the terminal alkyloxy chain containing 1, 2 and 3 groups in a trans-conformation.

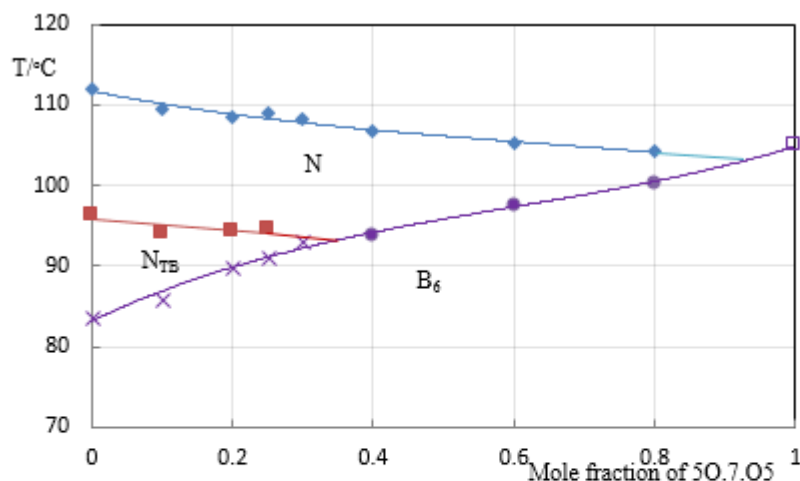


Figure 11. (colour online) The phase diagram for a mixture of the dimers 4O.7.O4 and 5O.7.O5 showing their miscibility in the B_6 phase across the entire composition range. Here \blacklozenge denotes the N-I transition, \blacksquare denotes the (N- N_{TB}) transition, \times denotes the (B_6 - N_{TB}) transition, \bullet denotes the (B_6 -N) transition and \square denotes the B_6 -I transition. The brackets () denote a monotropic transition.

3.1.7 Dimers *mO.11.Om*

We end this series of dimers with those having the longest spacer namely 11 methylene groups and so one for which the effect of flexibility should be particularly pronounced. The results for the transition temperatures are shown in Figure 12(a); all members of the series are seen to form enantiotropic nematic phases. This behaviour may result from the length of the spacer so that the inhomogeneity resulting from the terminal chains is minimised. Indeed the lamellar B_6 phase is only formed at a low temperature for the pentyloxy chain but just below the nematic phase for the hexyloxy chain and related to the $m > n/2$ rule. In addition the odd-even effect in the N-I transition temperatures is not as pronounced as for the *mO.7.Om* series (see Figure 9) with its shorter spacer which allows the terminal chains to have a greater relative effect on T_{NI} . The dimers do form the twist-bend nematic phase for terminal chain lengths of 1, 2 and 4; it would appear as though the dimer, with the terminal chain length of 3, should also form the twist-bend phase but despite numerous attempts it was not possible to stabilise this. As we had noticed previously for the shorter spacer, the N_{TB} -N transition temperature mimicked that for the N-I transition when the spacer length is constant. This is also true for the longer spacer where for terminal chain lengths of 1, 2 and 4 the differences in the transition temperatures are 29, 29 and 25°C which compare with 22, 24 and 16°C for the same terminal chain lengths in the *mO.7.Om* series. These differences appear to result from a higher value of the T_{NI} for the *mO.11.Om* series which is an interesting result. As we have noted the optical textures played an important role in this study when identifying the phases formed and in Figure 13 we show those for the dimer 2O.11.O2 in the nematic and twist-bend nematic phases, at 103.4°C and 81.6°C,

respectively. The nematic phase is identified by its Schlieren texture and the twist-bend nematic phase by its striking stripe- and rope-like textures.

The transitional entropies are characterised by two extremes as the results in Figure 12(b) demonstrate. First the small values measured for the N_{TB} -N transitions are presumably related to the long spacer while at the other extreme are the results for the two dimers with the longest terminal chains. These exhibit the B_6 -N transition and with the lamellar structure have a relatively large value but not so large as for the shorter spacer $mO.3.Om$ dimers indicating a smaller order for the B_6 phase. In between these two extremes are the results for the N-I transition which are similar in form to those for $mO.7.Om$ (see Figure 9(b)) but somewhat larger; this is presumably related to the larger anisotropy produced by the long spacer.

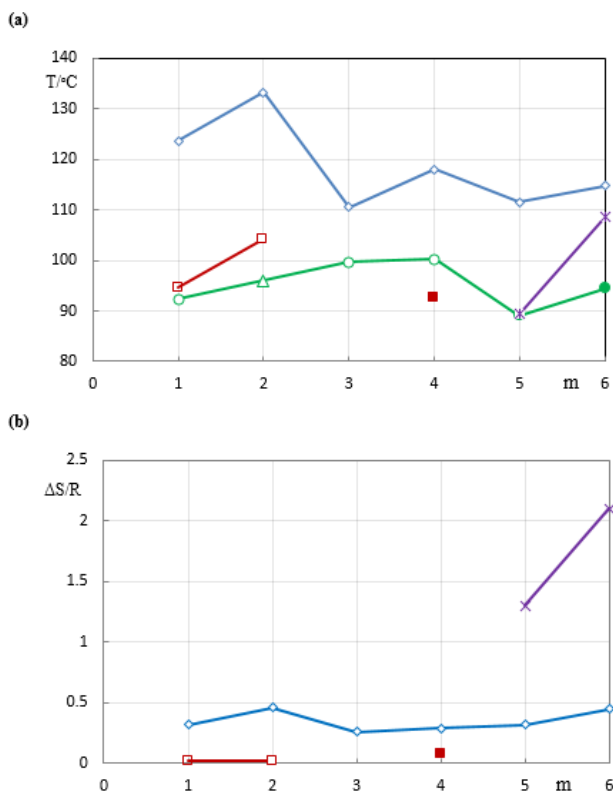
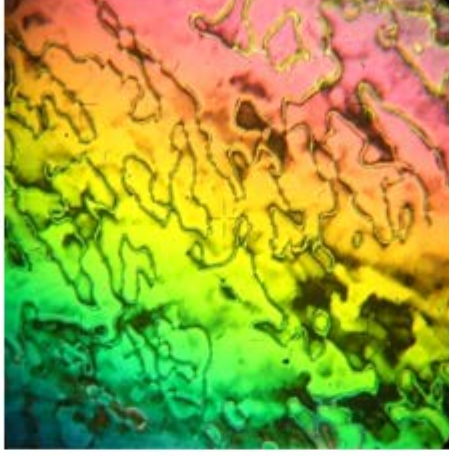


Figure 12. (colour online) The dependence of (a) the transition temperatures, T_i , and (b) the scaled transitional entropies, $\Delta S/R$, on the number of carbon atoms, m , in the terminal alkyloxy chains for the dimers $mO.11.Om$. The symbols used to denote the transition temperatures and transitional entropies are \bullet for $Cr-B_6$; Δ for $Cr-N_{TB}$; \circ for $Cr-N$; \times for B_6-N ; \square for $N_{TB}-N$; \blacksquare for $(N_{TB}-N)$; \diamond for N-I.

(a)



(b)

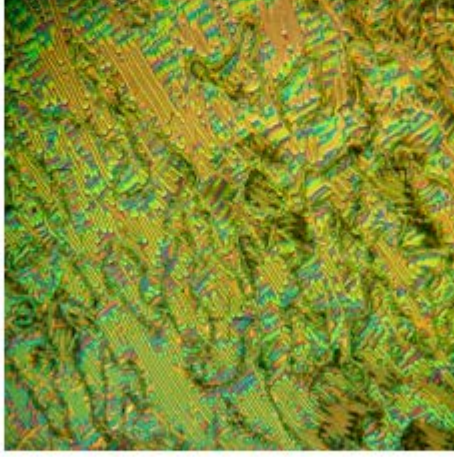


Figure 13. The optical textures exhibited by the dimer 2O.11.O2 on cooling from the isotropic phase showing (a) the Schlieren texture of the N phase at 103.4 °C and (b) the rope-like and stripe-like texture of the N_{TB} phase at 81.6 °C.

4. Properties

4.1 X-ray scattering

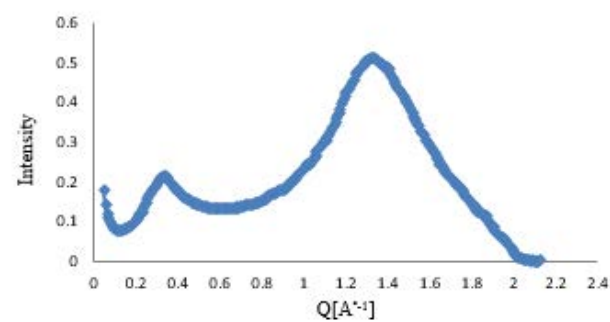
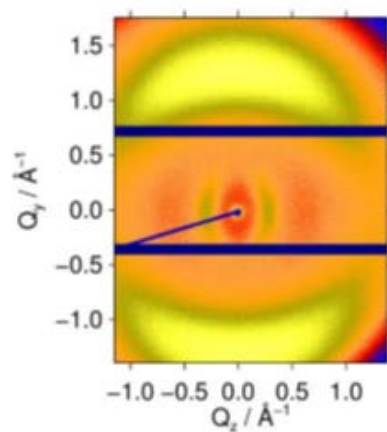
As for previous studies of twist-bend nematics X-ray scattering has been employed to explore the structure and orientational order of the nematic phases [12,21,45]. Here we consider the N and N_{TB} phases of the dimer 2O.7.O2 both of which are enantiotropic (see Table 3). The nematic phase was aligned for this by the application of a 1T magnetic field which is more than sufficient and because the diamagnetic anisotropy is positive the director is aligned parallel to the field. In contrast this field strength is insufficient to align the N_{TB} phase directly but this can be achieved by first aligning the nematic and then carefully lowering the temperature in the presence of the field until in the N_{TB} at which point the helix axis is aligned parallel to the magnetic field [46].

The X-ray scattering pattern of the N phase at 120°C is shown in Figure 14(a) where the small- and wide-angle arcs are clearly apparent and demonstrate the macroscopic order of the phase. The location of the arcs in Q-space is shown by the azimuthally averaged scattering intensity around the arcs from the centre $Q = 0$ until the outer edge at 2.2 \AA^{-1} of the scattering pattern. The maximum in the wide-angle region occurs when Q is 1.33 \AA^{-1} corresponding to a local side-by-side separation between mesogenic dimers of 4.7 \AA which is comparable to that observed for monomers such as the 4-alkyloxy-4'-cyanobiphenyls. The single small-angle peak at Q of 0.33 \AA^{-1} corresponds to a local end-to-end separation of about 19 \AA . Quantum chemical calculations *in vacuo* give the molecular length in the ground state as about 34 \AA , and so the ratio of separation to length is approximately 0.54 as might be expected for a local intercalated structure often observed for the N_{TB} phase [2, 12, 21].

In the N_{TB} phase the positions of the maxima in the azimuthally averaged scattering are essentially the same as those in the N phase. This means, therefore, that in the N_{TB} phase the local structure might also be viewed as intercalated. This would certainly be in keeping with X-ray scattering studies of other liquid crystal dimers forming the twist-bend nematic phase. In addition this structure would be consistent with the observation that for some systems the N_{TB} phase undergoes a transition to a B_6 phase whose lamellar phase is also intercalated. The diffuse nature of the small-angle arcs shown in Figure 14(b) is again in keeping with investigations of the N_{TB} phase of other dimers, not a smectic structure but certainly a nematic.

The other change in the scattering pattern on passing from the nematic to the twist-bend nematic phase is that the extent of the wide-angle arcs increases. This growth has been found for other X-ray studies of the N to N_{TB} transition [3,11]. Such an increase could be associated with a decrease in the orientational order of the twist-bend nematic phase but for this analysis to hold the macroscopic order of the two nematic phases should remain unchanged. However this is difficult to discern from the scattering patterns alone. To do so would, for example, require the measurements to be made for a series of field strengths, preferably increasing but possibly decreasing. We should note that in an early ESR study of the dimer CB7CB it was discovered that although the field of 0.3T was sufficient to align the director of the nematic phase, as is to be expected, on lowering the temperature into the N_{TB} the ESR spectrum changed in such a way as to indicate that the director was no longer uniformly aligned [12]. Whether such behaviour occurs for the dimer 2O.7.O2 is not certain. Clearly more studies are required to demonstrate that the N_{TB} aligned from the N phase by a magnetic field of 1T is perfectly aligned.

(a)



(b)

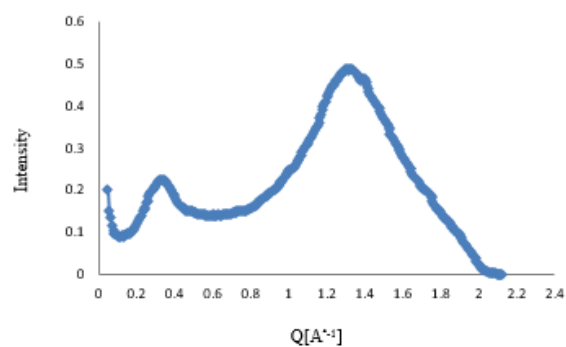
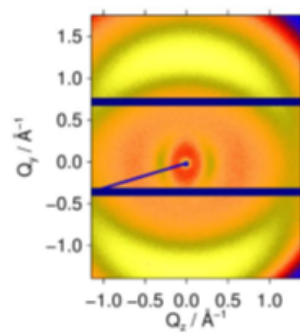


Figure 14. (colour online) X-ray scattering patterns of the aligned 2O.7O2 dimer in (a) the nematic phase at 110 °C together with the associated Q -dependent azimuthally averaged scattering intensity and (b) the twist-bend nematic phase at 105 °C again with the azimuthally averaged scattering intensity.

4.2 ^2H NMR spectroscopy

4.2.1 Methodology

^2H NMR spectroscopy has played a significant role in the identification of the twist-bend nematic phase for CB7CB- d_4 [12] and subsequently for other dimers [46-48]. The basis of this methodology is not perhaps so well-known and so we introduce it briefly here [49]. The ^2H NMR spectrum of a nematogen whose molecules possess a single deuteron contains a single line. However in the nematic phase, aligned by the magnetic field of the NMR spectrometer, the single peak is split into a doublet by the residual quadrupolar splitting of the deuteron. In a molecule, such as the dimer CB7CB- d_4 , where two of the deuterons are in the first methylene group of the heptane spacer and the other two are in seventh methylene group the spectral situation is more interesting. The deuterons in each of the methylene groups are known as prochiral and are equivalent because of the mirror plane relating them. Consequently the ^2H NMR spectrum in the nematic phase still contains a single doublet because of this equivalence and that relating the groups at the two ends of the spacer. However in the twist-bend nematic the phase chirality removes the plane of symmetry and hence the equivalence of the prochiral deuterons is lost. The spectrum therefore contains two quadrupolar doublets having equal intensities [50-52]. The N_{TB} phase is strictly a conglomerate composed of degenerate domains having opposite handedness although this is not apparent from the spectrum but can be discerned. The difference in the two splittings is related to the phase chirality and invariably grows with decreasing temperature [46, 47]. On the other hand the mean of the splittings is related to the quadrupolar splitting observed in the nematic phase.

4.2.2 Dimer 2O.7.O2

Formally, of course, all of the dimers contain deuterium but most only in natural abundance which is at an insufficient level for the spectrometer available to us. To overcome this problem we have added prochiral deuterons in the form of a spin probe and for our investigation we used CB7CB- d_4 with which we have some experience. We have studied many of the *mO.n.Om* dimers but here we use the dimers 2O.7.O2, 4O.7.O4 and 6O.7.O6 as exemplars. The amount of the probe used to study 2O.7.O2 was of the order of 3wt% which is sufficiently small that the properties of the host dimer are not altered to any significant extent. The NMR spectrum in the nematic phase of 2O.7.O2 at 102°C is shown in Figure 15(a); it contains a single quadrupolar doublet having relatively sharp spectral lines. On lowering the temperature sample deep into the twist-bend nematic phase to 86.5°C the spectrum is found, as expected, to contain two quadrupolar doublets which are shown in Figure 15(b). The intensities of the two doublets are similar but not quite identical which comes from an instrumental effect.

However what is apparent is that there are two doublets in the N_{TB} phase as opposed to one in the N phase demonstrating the chirality of the twist-bend nematic phase in keeping with its structure.

As the temperature changes so the quadrupolar splitting for the deuterons on a methylene carbon, $\Delta\nu_{CD}$, also alter and how this occurs is apparent from the plot of the splittings against the shifted temperature, $(T_{NI}-T)$, shown in Figure 16. What is seen is that $\Delta\nu_{CD}$ jumps from zero in the isotropic phase to non-zero in the nematic in keeping with the first-order character of the N-I transition. The rate at which the splitting grows decreases as the transition to the N_{TB} phase approaches in keeping with the orientational order of the probe in the phase. To a good approximation $\Delta\nu_{CD}$ is proportional to the Saupe order parameter for the C-D bond. However, to obtain the order parameter, S_{ZZ} , for the p-axis of the cyanobiphenyl group which has perhaps greater significance it is necessary to include the biaxiality of the mesogenic group. This requires at least one additional piece of information. Since this is not available from our 2H NMR experiments it is necessary to neglect the biaxiality which gives S_{ZZ} as

$$S_{ZZ} \approx 2\Delta\nu_{CD}(\text{kHz}) / 3 \times 168(\text{kHz}) P_2(\cos \theta), \quad (1)$$

where θ is the angle between the C-D bond and the p-axis which is taken to be 109° and the quadrupolar coupling constant is taken as 168kHz [12,46]. Substituting these values in Equation (1) gives

$$S_{ZZ} \approx 0.01164(\text{kHz}) \Delta\nu_{CD}(\text{kHz}). \quad (2)$$

From the splittings it seems that in the nematic phase the order parameter grows from about 0.27 at T_{NI} to about 0.51 just before the transition to the N_{TB} phase; these values are comparable to those found for CB7CB-d₄ itself with which it shares a seven membered spacer. Within the N_{TB} phase the mean splitting shown in Figure 16 exhibits a small jump at the N_{TB} -N transition and then grows slightly at a rate comparable to that for the last four points in the nematic phase. This slight growth in $\Delta\nu_{CD}$ suggests that the increasing contribution from the orientational order is greater than the decreasing contribution from the increase in the conical angle, one of the defining parameters for the N_{TB} phase [53]. Finally it is of interest to evaluate the order parameters from Equation (2) remembering that these are defined with respect to the helix axis which in our experiments is aligned parallel to the magnetic field of the spectrometer. As we noted, the order parameter at the start of the N_{TB} phase is to within experimental error the same as that at the end of the nematic, namely 0.51. At the end of the twist-bend nematic phase this has only grown to 0.56, comparable to that for CB7CB-d₄ [12].

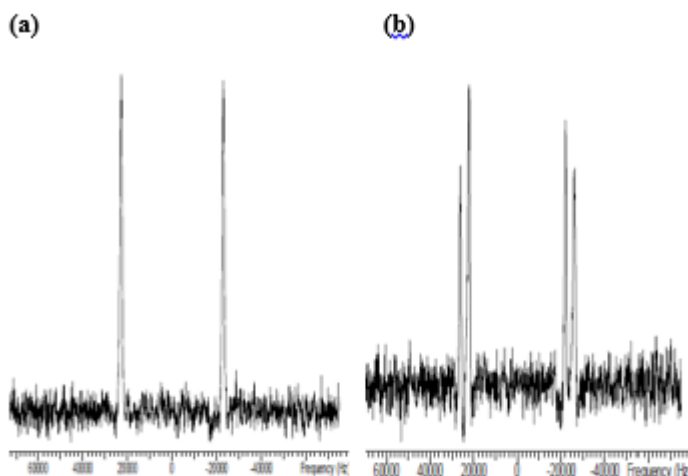


Figure 15. The ^2H NMR spectra of 2O.7.O2 doped with 3wt % CB7CB- d_4 (a) in the N phase at 102 °C and (b) in the N_{TB} phase at 86.5 °C.

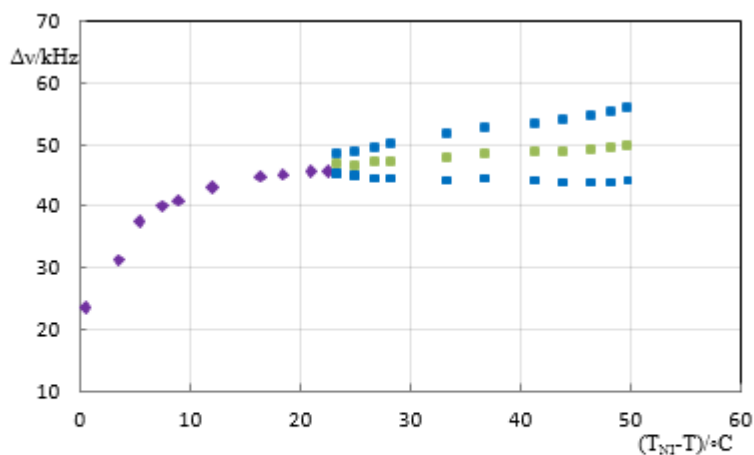


Figure 16. (colour online) The dependence of the quadrupolar splittings, $\Delta\nu_{\text{CD}}$, on the shifted temperature $(T_{\text{NT}} - T)$ for 2O.7.O2 doped with 3wt % CB7CB- d_4 . Here \blacklozenge denotes the quadrupolar splitting in the nematic phase, \blacksquare denotes the two quadrupolar splittings in the N_{TB} phase and \blacksquare denotes the mean of these two quadrupolar splittings in the N_{TB} phase.

4.2.3 Dimer 4O.7.O4

4O.7.O4 is the second dimer with a seven spacer that we have studied using ^2H NMR. Here the choice was prompted by the phase sequence it exhibits, $\text{Cr} - \text{B}_6 - \text{N}_{\text{TB}} - \text{N} - \text{I}$, even though both the B_6 and N_{TB} phase are monotropic. One of our aims was to investigate the B_6 phase following the N_{TB} phase to look for similarities between the local order of the latter and the long-range order of the former. It is also of interest to confirm the expected achirality of the B_6 phase. As with previous experiments the dimer was doped with CB7CB- d_4 , 3.4wt%.

The spectra observed for the N phase consisted of a single quadrupolar doublet and in the N_{TB} phase this became two doublets thus demonstrating the chirality of the phase formed by 4O.7.O4. The study of the twist-bend nematic phase was possible because this could be supercooled within in the spectrometer from the enantiotropic nematic phase. However, despite the success with the N_{TB} phase it did not prove possible to supercool the sample in the B_6 phase; this always crystallised despite numerous attempts to prevent it. We were not able therefore to demonstrate the achirality of the B_6 phase but we shall return to this phase in the following section.

The quadrupolar splittings that we were able to determine for the spin probe in the dimer are shown as a function of the shifted temperature ($T_{NI} - T$) in Figure 17. Δv_{CD} in the nematic phase grows relatively rapidly from 23 kHz at the N-I transition to 43 kHz just before the N_{TB} phase is formed. The nematic range for 4O.7.O4 is significantly less than that for 2O.7.O2 and it is this difference which is responsible for the larger jump to the mean splitting at the transition to the N_{TB} phase. This is also consistent with the larger transitional entropy, $\Delta S_{N_{TB}N}/R$, for 4O.7.O4 in comparison with the earlier homologue 2O.7.O2; behaviour in keeping with the analogue between the N_{TB} and SmA phases [22]. On entering the N_{TB} phase the mean splitting grows with decreasing temperature which, as for 2O.7.O2, indicates that the growth in the conical angle is insufficient to overcome the contribution to Δv_{CD} originating from the orientational order of the phase [53]. The difference in the prochiral splittings which is related to the phase chirality grows from a non-zero value at the $N_{TB} - N$ transition. At a quantitative level the chiral splitting is proportional to an off-diagonal element of the Saupe ordering matrix evaluated in a frame set in one of the two deuteriated methylene groups [46]. Rather than pursue this issue further here we shall consider the order parameters evaluated from Δv_{CD} in both the nematic and twist-bend nematic phase. First, at the N-I transition the order parameter, S_{ZZ} , obtained from Equation (2) is 0.27 and at the end of the nematic phase it has grown to 0.50. These values are comparable to those for the spin probe in 2O.7.O2 and also for CB7CB-d₄ itself. In the N_{TB} phase the order parameter, now measured with respect to the helix axis, is 0.52 and at the end of the phase it has grown to just 0.57. Again these values are, at comparable temperatures, equal to those for the probe in both 2O.7.O2 and CB7CB-d₄ [12] although both of these have longer, albeit supercooled, N_{TB} ranges.

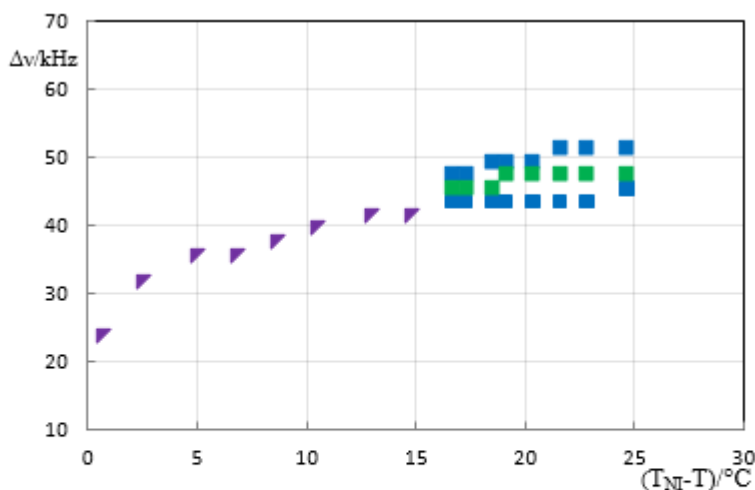


Figure 17. (colour online) The dependence of the quadrupolar splittings, $\Delta\nu_{CD}$, on the shifted temperature $(T_M - T)$ for 4O.7.O4 doped with 3.4wt % CB7CB-d₄. Here ♦ denotes the quadrupolar splitting in the nematic phase, ■ denotes the two quadrupolar splittings in the N_{TB} phase and ■ denotes the mean of these two quadrupolar splittings in the N_{TB} phase.

4.2.3 Dimer 6O.7.O6

This last dimer was chosen not only because it has a heptane spacer but, more importantly, because it forms an enantiotropic B₆ phase directly from the isotropic phase. The dimer was doped with 2.7wt% of CB7CB-d₄ and it proved possible to align it in the B₆ phase; the sharpness of the spectral lines suggests that the director alignment by the magnetic field was essentially complete. On lowering the temperature there is a small biphasic region of $\sim 1.5^\circ\text{C}$ in which the B₆ and isotropic phase coexist in keeping with the first-order nature of the transition with its large transitional entropy (see Table A3). Since the magnetic field of the spectrometer is high, at 9.40T, the alignment of the lamellar B₆ is not surprising although curiously the alignment of the N_{TB} phase by such a field is not so facile. Apart from the small biphasic region where both a single central line and a quadrupolar doublet coexist the subsequent spectra contain a single doublet at temperatures about 10°C below the freezing point. The observation of just a single doublet confirms the achirality of the B₆ phase. The quadrupolar splitting, $\Delta\nu_{CD}$, measured from this is shown in Figure 18 as a function of the shifted temperature, $(T_{B_6} - T)$. The quadrupolar splitting starts at 63 kHz which is relatively large and then over the range of the B₆ changes linearly by just a few kHz. This behaviour is in keeping with that expected for a smectic A phase formed directly from an isotropic phase. The order parameter for the spin probe in the 6O.7.O6 dimer is large being of the order of 0.73, especially when allowance is made for the biaxiality of the probe and the associated tilt of its mesogenic arms.

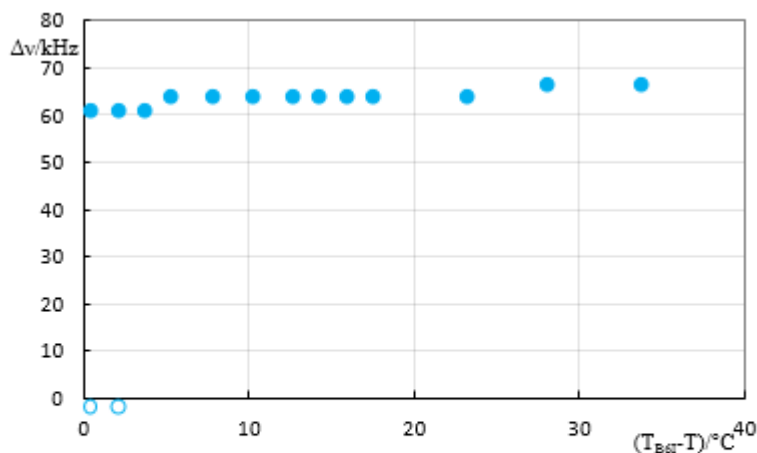


Figure 18. (colour online) The dependence of the quadrupolar splitting, $\Delta\nu_{\text{CD}}$, on the shifted temperature $(T_{B6T} - T)$ for 6O.7.O6 doped with 2.7wt % CB7CB- d_4 . Here \circ indicates the isotropic peak in the biphasic region and \bullet denotes the quadrupolar splitting in the biphasic region and across the B_6 phase.

5. Conclusions

The expectation that the twist-bend nematic phase could emerge from the isotropic phase was stimulated by the analogy between the smectic A phase and the N_{TB} phase as well as by the predictions of the extended molecular field theory. In the attempt to locate this novel phase transition it was decided to create a range of liquid crystal dimers whose structures could be changed systematically. Based on the benzyloxybenzylidene group we had prepared dimers where both the spacer length and that of the terminal alkyloxy chains were varied. With this approach we found just two dimers, 1O.3.O1 and 2O.3.O2, which exhibited the $N_{\text{TB}} - \text{I}$ transition albeit monotropic. In fact the stabilisation of the N_{TB} phase proved to be challenging but with perseverance achievable. Having other homologues of the series available allowed us to see that it is the reduction in T_{NI} rather than an increase in T_{NtbN} which resulted in the observation of the N_{TB} formed directly from the isotropic phase.

The creation of a wealth of homologues in both spacer and terminal chains has allowed the examination as to how these molecular features influence the transitional properties of the dimers; first varying the spacer whilst keeping the terminal chain fixed is addressed. The variation of T_{NI} for the odd dimers exhibits an interesting increase but then passes through a maximum. Such behaviour has been well-understood by molecular field theory which allows for the spacer flexibility. This is of real value since the change in $T_{\text{N}_{\text{TB}}\text{N}}$ along some series is found to parallel that of T_{NI} which might lead to a more realistic description of the factors influencing this transition. The $N_{\text{TB}} - \text{N}$ transition is first order for these dimers and the varying entropy change will provide a real challenge for theories to predict. Part of the treasure trove of data is the transitional properties of the homologues where the spacer length is fixed and the terminal chain length varies. For those series which contain $\text{N} - \text{I}$ and $N_{\text{TB}} - \text{N}$

transitions the temperatures exhibit a strong odd-even effect which resemble those of monomers with comparable chains. Qualitatively this behaviour is related to the anisotropy of the mesogenic groups but again molecular field theory offers a better path to understanding the transitional behaviour. The other feature of the terminal chain is the introduction of the B₆ into the phase behaviour occasionally following the N_{TB} phase; the interaction between these is of some interest.

The X-ray experiments are of special interest when the dimer exhibits both nematic and twist-bend nematic phases partly to confirm the phase identification and to show the intercalation of the local structure. This seems to be consistent with the macroscopic intercalated structure of the B₆ phase. Of equal interest is the increase in the breadth of the wide-angle arcs on passing from the N to the N_{TB} phase. What are needed now are further studies to clarify the macroscopic state of the N_{TB} phase.

²H NMR spectroscopy clearly provides a valuable tool to demonstrate the chirality or its absence in a phase. It also provides a realistic route to the orientational order parameter and the conical angle which are defining parameters for the twist-bend nematic phase. For example, the order parameters for dimers with heptane spacers but different rod-like mesogens are similar and the results suggest that the influence of the conical angle on the splittings is less than that of the orientational order. Indeed it is possible to determine the conical angle from these ²H NMR experiments. In addition the factor reflecting the phase chirality and how it varies with temperature can be explored. However, the molecular complexity of the liquid crystal dimers forming the N_{TB} phase strictly require experiments with a higher information content than that given by CB7CB-d₄. This could be provided by more extensive specific deuteration of the dimers but other magnetic nuclei, such as ¹H and ¹³C, also provide a valuable and accessible route to the residual magnetic tensors needed to determine the order and structure of the dimers. The availability of structurally related liquid crystal dimers will surely aid in the determination of key properties of the twist-bend nematic phase.

Acknowledgements

We are grateful to a number of colleagues who have helped us with this project. They are Mr Herbert Zimmermann of the Max-Planck-Institut für Medizinische Forschung, Heidelberg for the sample of CB7CB-d₄; Professor Corrie Imrie of the University of Aberdeen for allowing us to measure optical textures of certain dimers; Professor Ghazwan Faisal of the University of Duhok for assistance with the calculations of the chemical structure and dimensions of the dimers and Mr Kevin Adlem of Merck Chemicals for allowing us to use their DSC equipment.

Disclosure statement

No potential conflict of interest was reported by the authors.

Funding

The Ganesha X-ray scattering apparatus used for this research was purchased under an EPSRC Grant “Atoms to Applications” Grant ref. EP/K035746/1. We also wish to thank Zakho University for the award of a split-site PhD grant to Dr Alya Dawood.

References

- [1] Ungar G. Percec V. Zuber M. Liquid crystalline polyethers based on conformational isomerism.20. Nematic-nematic transition in polyethers and copolyethers based on 1-(4-hydroxyphenyl)2-(2-R-4-hydroxyphenyl)ethane with R = fluoro, chloro and methyl and flexible spacers containing an odd number of methylene units. *Macromol.* 1992; 25:75-80.
- [2] Šepelj M. Lesac A. Baumeister U. Diele S. Nguyen HL. Bruce BW. Intercalated liquid- crystalline phases formed by symmetric dimers with an α,ω -diiminoalkylene spacer. *J Mat Chem.* 2007; 17: 1154-1165.
- [3] Panov VP. Nagaraj M. Vij JK. Panarin VP. Kohlmeier A. Tamba MG. Lewis RA. Mehl GH. *Phys Rev Lett.* 2010; 105: 167801
- [4] Tripathi CSP. Losada-Pérez P. Glorieux C. Kohlmeier A. Tamba M-G, Mehl GH. Leys J. Nematic-nematic phase transitions in the liquid crystal dimer CBC9CB and its mixtures with 5CB: A high-resolution adiabatic scanning calorimetric study. *Phys Rev E.* 2011;84: 041707 .
- [5] Meyer RB. Structural problems in liquid crystal physics, Les Houches Summer School in Theoretical Physics. 1973 Molecular Fluids, eds. Balian R. Weil G., Gordon and Breach, New York 1976: 273-373.
- [6] Dozov I. On the spontaneous symmetry breaking in the mesophases of achiral banana-shaped molecules. *Europhys Lett.* 2001; 56:247-253.
- [7] Chen D. Porada JH. Hooper JB. Klitnick A. Shen Y. Tuchband MR. Korblova E. Bedrov D. Walba DM. Glaser MA. MacLennan JE. Clark NA. Chiral heliconical ground state of nanoscale pitch in a nematic liquid crystal of achiral molecular dimers. *PNAS.* 2013;110:15931.
- [8] Borshch V. Kim Y-K. Xiang J. Gao M. Jákli A. Panov VP. Vij JK. Imrie CT. Tamba MG. Mehl GH. Lavrentovich OD. Nematic twist-bend phase with nanoscale modulation of molecular orientation. *Nature Comm.* 2013;4:2635 .
- [9] Greco C. Luckhurst GR. Ferrarini A. Enantiotopic discrimination and director organization in the twist-bend nematic phase. *Phys Chem Phys Chem.* 2013;15:14961-14965.
- [10] Chen D. [Nakata M.](#) [Shao R.](#) [Tuchband MR.](#) [Shuai M.](#) [Baumeister U.](#) [Weissflog W.](#) [Walba DM.](#) [Glaser MA.](#) [MacLennan JE.](#) [Clark NA.](#) Twist-bend heliconical chiral nematic liquid crystal phase of an achiral rigid bent-core mesogen. [Phys Rev E Stat Nonlin Soft Matter Phys.](#) 2014; 89:022506.

- [11] Wang Y. Singh G. Agra-Kooijman DM. Gao M. Bisoyi HK. Xue C. Fisch MR. Kumar S. Li Q. Room temperature heliconical twist-bend nematic liquid crystal. *CrystEngComm*. 2015;17:2778-2782.
- [12] Cestari M. Diez-Berart S. Dunmur DA. Ferrarini A. de la Fuente MR. Jackson DJB. Luckhurst GR. Perez-Jubindo MA. Richardson RM. Salud J. Timimi BA. Zimmermann H. Phase behavior and properties of the liquid-crystal dimer 1'',7''-bis(4-cyanobiphenyl-4'-yl) heptane: A twist-bend nematic liquid crystal. *Phys Rev. E* 2011; 84:031704.
- [13] Dong RY. Kohlmeier A. Tamba MG. Mehl GH. Burnell EE. Solute NMR study of a bimesogenic liquid crystal with two nematic phase. *Chem Phys Lett*. 2012; 552: 44-48.
- [14] Šepelj M. Baumeister U. Ivšić T. Lesac A. Effects of geometry and electronic structure on the molecular self-assembly of naphthyl-based dimers. *J. Phys Chem B*. 2013;117:8918-8929.
- [15] Henderson PA. Imrie CT. Methylene-linked liquid crystals and the twist-bend nematic phase. *Liq Cryst*. 2011;38:1407-1414.
- [16] Mandle RJ. Davis EJ. Archbold CT. Voll CCA. Andrews JL. Cowling SJ. Goodby JW. Apolar mesogens and the incidence of the twist-bend nematic phase. *Chem Eur J*. 2015; 21:8158-8146.
- [17] Mandle RJ. The dependence of twist-bend nematic liquid crystals on molecular structure from dimers to trimers and polymers. *Soft Matt*. 2016;12:7883-7901.
- [18] Mandle RJ. Davis EJ. Lobato SA. Voll CCA. Cowling SJ. Goodby JW. Characterisation of an unsymmetrical, ether-linked, fluorinated bimesogen exhibiting a new polymorphism containing the N_{TB} or 'Twist-Bend' phase. *Phys Chem Chem Phys*. 2014;16:6907-6915.
- [19] Sebastián N.. López DO, Robles-Hernández B. de la Fuente MR. Salud J. Perez-Jubindo MA., Dunmur DA. Luckhurst GR. DJB. Jackson. Dielectric, calorimetric and mesophase properties of 1''-(2',4-difluorobipenyl-4'-yloxy)-9''-(4-cyanobiphenyl-4'-yloxy) nonane: an odd liquid crystal dimer with a monotropic mesophase having the characteristics of a twist-bend nematic phase. *Phys Chem Chem Phys*. 2014; 16: 21391- 21407.
- [20] Mandle RJ. Voll CCA. Lewis DJ. Goodby JW. Etheric bimesogens and the twist-bend nematic phase. *Liq Cryst*. 2016;43:13-21.
- [21] Paterson DA. Gao M. Kim Y-K. Jamali A. Finley K. Robles-Hernández B. Diez-Berart S. J. Salud, de la Fuente MR. Timimi BA. Zimmermann H. Greco C. Ferrarini A. Storey JMD. López DO. Lavrentovich OD. Luckhurst GR. Imrie CT. Understanding the twist-bend nematic phase: the characterisation of 1-(4-cyanobiphenyl-4'-yloxy)-6-(4-cyanobiphenyl-4'-yl) hexane (CB6OCB) and comparison with CB7CB. *Soft Matt*. 2016;12:6827-6840.
- [22] Imrie CT. Luckhurst GR. Liquid crystal dimers and oligomers. In Goodby JW. Collings PJ. Kato T. Tschierske C. Gleeson HF. Raynes P. Editors. *Handbook of liquid crystals* 2nd Edition, Wiley-VCH, Weinheim, Germany, 2014, Vol 7 part II.
- [23] Meyer C. Luckhurst GR. Dozov I. Flexoelectrically driven electroclinic effect in the twist-bend nematic phase of achiral molecules with bent shapes. *Phys Rev Lett*. 2013;111: 067801.

- [24] Greco C. Luckhurst GR. Ferrarini A. Molecular geometry, twist-bend nematic phase and unconventional elasticity: a generalised Maier-Saupe theory. *Soft Matter*. 2014; 10: 9318-9323.
- [25] Archbold CT. Davis EJ. Mandle RJ. Cowling SJ. Goodby JW. Chiral dopants and the twist-bend nematic phase – induction of novel mesomorphic behaviour in an apolar bimesogen. *Soft Matter*; 2015;11:7547-7557.
- [26] Dawood AA. Grossel MC. Luckhurst GR. Richardson RM. Timimi BH. Wells NJ. Yousif YZ. On the twist-bend nematic phase formed directly from the isotropic phase. *Liq Cryst*. 2016; 43: 2-12.
- [27] Thaker BT. Patel P. Vansadia AD. Patel HG. Synthesis, characterisation, and mesomorphic properties of new liquid-crystalline compounds involving ester-azomethine central linkages and a thiazole ring. *Mol Cryst Liq Cryst*. 2007;466: 13-22.
- [28] Dawood AA. The twist-bend nematic phase and liquid crystals dimers. Doctoral Thesis. University of Zakho. Kurdistan Regional Government, Iraq. 2015.
- [29] McMillan WL. Simple molecular model for the smectic A phase of liquid crystals. *Phys Rev A*. 1971;4:1238-1244.
- [30] Emsley JW. Luckhurst GR. Shilstone GN. Sage I. The preparation and properties of the α,ω -bis(4,4'-cyanobiphenyloxy)alkanes nematogenic molecules with a flexible core. *Mol Phys Liq Cryst Lett*. 1984;102:223-233.
- [31] Luckhurst GR. Liquid crystals: a chemical physicist's view. *Liq Cryst*. 2005;32:1335-1364.
- [32] Flory PJ. Statistical physics of chain molecules. Wiley, New York. 1969.
- [33] Ryckaert JP. Bellemans A. Molecular dynamics of liquid n-butane near its boiling point. *Chem Phys Lett*. 1975 ;30 :123-125.
- [34] Ferrarini A. Luckhurst GR. Nordio PL. Odd-even effects in liquid crystal dimers with flexible spacers: a test of the rotational isomeric state approximation? *Mol Phys*. 1995;85:131-143.
- [35] Henderson PA. Niemeyer O. Imrie CT. Methylene-linked liquid crystal dimers. *Liq Cryst*. 2001;28: 463-472.
- [36] Emerson APJ. Luckhurst GR. On the relative propensity of ether and methylene linkages for liquid crystal formation in calamitics. *Liq Cryst*. 1991; 10: 861-868.
- [37] Lopez DO. Robles-Hernandez B. Salud J. de la Fuente MR. Sebastian N. Diez-Berart S. Jaen X. Dunmur DA. Luckhurst GR. Miscibility studies of two twist-bend nematic liquid crystals with different average molecular curvature. A comparison between experimental data and predictions of a Landau mean-field theory for the $N_{TB} - N$ phase transition. *Phys Chem Chem Phys*. 2016;18:4394-4404.
- [38] Pelzl G. Diele S. Weissflog W. Banana-shaped compounds – a new field of liquid crystals. *Adv Mater*. 1999;11: 707-724.

- [39] Roullion JC. Marcerou JP. Laguerra M. Nguyen HT. Achard MF. New banana-shaped thiobenzoate liquid crystals with B₆, B₁ and B₂ phases. *J Mat Chem*. 2001;11:2946-2950.
- [40] Weissflog W. Wirth I. Diele S. Pelzl G. Schmalfuss H. Schoss T. Würflinger A. The N,N'-bis[4-(4-*n*-alkyloxybenzoyloxy)benzylidene]-phenylene-1,3-diamines: mesophase behaviour and physical properties. *Liq Cryst*. 2001;28:1603-1609.
- [41] Date RW. Imrie CT. Luckhurst GR. Seddon JM. Smectogenic dimeric liquid crystals. The preparation and properties of the α,ω -bis(4-*n*-alkylanilinebenzylidene-4'-oxy)alkanes. *Liq Cryst*. 1992;12:203-238.
- [42] Gray GW. Mosley A. Trends in the nematic-isotropic liquid transition temperatures for the homologous series of 4-*n*-alkyloxy- and 4-*n*-alkyl-4'-cyanobiphenyls. *J Chem Soc Perkin Trans 2*. 1976:97-102.
- [43] Marčelja S. Chain ordering in liquid crystals. I. Even-odd effect. *J Chem Phys*. 1974;60:3599-3604.
- [44] Jin JI. Oh HT. Park JH. Thermotropic compounds having two terminal mesogenic units and central spacers. Part 9. Homologous α,ω -bis-[p-(4-alkyloxy phenoxy)carbonyl]phenoxy]alkanes. *J Chem Soc Perkin Trans II*. 1986: 343-347.
- [45] Singh G. Agra-Kooijman DM. Fisch MR. Vengatesan MR. Song J-K. Kumar S. Orientational order in the nematic and heliconical nematic liquid crystals. arXiv: 1510.08362v1.
- [46] Beguin L. Emsley JW. Lelli M. Lesage A. Luckhurst GR. Timimi BA. Zimmermann H. The chirality of a twist-bend nematic phase identified by NMR spectroscopy. *J Phys Chem B*. 2012; 116: 7940-7951.
- [47] Robles-Hernández B. Sebastián N. de la Fuente MR. López DO. Diez-Berart S. Salud J. Blanca Ros M. Dunmur DA. Luckhurst GR. Timimi BA. Twist, tilt and orientational order at the nematic to twist-bend nematic phase transition of 1'',9''-bis(4-cyanobiphenyl-4'-yl) nonane (CB9CB): a dielectric, ²H NMR and calorimetric study. *Phys Rev E*. 2015;92:062505.
- [48] Adlem K. Čopič M. Luckhurst GR. Mertelj A. Parri O. Richardson RM. Snow BD. Timimi BA. Tuffin RP. Wilkes D. Chemically induced twist-bend nematic liquid crystals, liquid crystal dimers and negative elastic constants. *Phys Rev E*. 2013; 88: 022503.
- [49] Emsley JW, editor. *Nuclear Magnetic Resonance of Liquid Crystals*, Reidel Publishing Company. 1985.
- [50] Czarniecka K. Samulski ET. Polypeptide liquid crystals: A deuterium NMR study. *Mol Cryst Liq Cryst*. 1981;63: 205-214.
- [51] Merlet D. Loewenstein A. Smadja W. Courtieu J. Lesot P. Quantitative description of the facial discrimination of molecules containing a prochiral group by NMR in a chiral liquid crystal. *J Am Chem Soc*. 1998;120:963-969.
- [52] Merlet D. Emsley JW. Lesot P. Courtieu J. The relationship between molecular symmetry and second-rank orientational order parameters for molecules in chiral liquid crystalline solvents. *J Chem Phys*. 1999 ;111: 6890-6896 .

- [53] Jokisaari JP. Luckhurst GR. Timimi BA. Zhu J. Zimmermann H. Twist-bend nematic phase of the liquid crystal dimer CB7CB. Orientational order and conical angle determined by ^{129}Xe and ^2H NMR spectroscopy. *Liq Cryst.* 2015; 42; 708-721.
- [54] Memmer R. Liquid crystal phases of achiral banana-shaped molecules: a computer simulation study. *Liq Cryst.* 2002;22:483-496.
- [55] Mandle RJ. Archbold CT. Sarju JP. Andrews JL. Goodby JW. The dependency of nematic and twist-bend mesophase formation on bend angle. *Sci Rep.* 2016;6:36682.
- [56] Emsley JW. Luckhurst GR. The effect of internal motion on the orientational order parameters for liquid crystalline systems. *Mol Phys.* 1980;41:16-29.
- [57] Emsley JW. Fung BM. Heaton NJ. Luckhurst GR. The potential of mean torque for flexible mesogenic molecules: Determination of the interaction parameters from carbon-hydrogen dipolar couplings for 4-n-alkyl-4'-cyanobiphenyls. *J Chem Phys.* 1987;87:3099-3103.
- [58] Luckhurst GR. Nematic liquid crystals formed from flexible molecules. Molecular field theory. In: Chapoy LL., editor *Recent advances in liquid crystalline polymers*. Chapter 7. Elsevier Applied Science Publishers; 1985.
- [59] Ferrarini A. Luckhurst GR. Nordio PI. Roskilly SJ. Prediction of the transitional properties of liquid crystal dimers. A molecular field theory calculation based on the surface tensor parametrization. *J Chem Phys.* 1994;100:1460-1469.
- [60] Luckhurst GR. Liquid crystal dimers and oligomers: experiment and theory. *Macromol Symp.* 1995;96:1-26.
- [61] Roskilly SJ. Molecular field theory of nematics composed of flexible molecules. PhD Thesis University of Southampton, United Kingdom. 1994.
- [62] Cestari, M. Frezza E. Ferrarini A. Luckhurst GR. Crucial role of molecular curvature of the bend elastic constant and flexoelastic properties of liquid crystals: mesogenic dimers as a case study. *J Mater Chem.* 2011; 21:12303-12308.
- [63] Yun CJ. Vengatesan MR. Vij JK. Song JK. Hierarchical elasticity of bimesogenic liquid crystals with twist-bend nematic phase. *App Phys Lett.* 2015;106:173102.
- [64] Balachandran R. Panov VP. Vij JK. Kocot A. Tamba MG. Kohlmeier A. Mehl GH. Elastic properties of bimesogenic liquid crystals. *Liq Cryst.* 2013; 40:681-688.

APPENDIX A: Molecular curvature, topology and the twist-bend nematic phase.

It has long been suspected if not known that the prime driving force for the creation of the twist-bend nematic phase, N_{TB} , is the curvature of the constituent molecules yielding not only biaxiality but also the shape polarity. Here we consider, at a qualitative level, how this can be estimated from the molecular structure and the optimum value needed to give the N_{TB} phase. Similar arguments apply to the splay-bend nematic phase but we shall not deal with them specifically in this Appendix.

At a particularly simple level the features required are contained in a rigid, V-shaped molecule with two uniaxial arms. This has the advantage that the curvature or bend of the molecule is related to the angle, χ , between the arms which vanishes when the angle is 0° and 180° ; in addition the shape polarity is zero. The simplicity of this idealistic molecule facilitates its theoretical study as a function of χ . For example, the generalised molecular field theory which incorporates the heliconical structure of the director has been employed in such an investigation [24]. What is found is that when χ is set equal to 140° the model is predicted to have a phase sequence $N_{TB} - N - I$. As expected when the angle is reduced slightly to 135° there is a reduction in the nematic range prior to the formation of the N_{TB} phase which proves to be significant, in fact by a factor of about 4.4. If the angle is reduced further to just 130° then the nematic phase is removed from the phase sequence and the isotropic phase undergoes a transition directly to the twist-bend nematic. We see that the phase and transitional behaviour are predicted to be extremely sensitive to the angle between the arms; that is to the molecular bend. It is of interest to note that a similar interarm angle of 140° was used in a Monte Carlo simulation of a V-shaped molecule based on two Gay-Berne particles which then formed a twist-bend nematic phase [54].

Armed with this information it is tempting to see how close these interarm angles are to that for liquid crystal dimers which form the N_{TB} phase. This should be related to the angle between the mesogenic arms of the dimer. An indication of this might be obtained from the angle between the long axes of the two mesogenic groups determined from Quantum Chemical calculations where the structure would be determined for the conformational ground state. Such calculations have been performed for the dimer CB9CB which has a $N_{TB} - N$ transition at 105.4°C and the angle χ is found to be 110.5° [55]. This is an interesting result which shows a significant difference with the predictions of the generalised molecular field theory that we have just described. The nonane chain seems to be in its all-*trans* form so that the ground state would not be a simple V but rather has a truncated-V shape. It might be expected that this would reduce the molecular bend in the dimer and it would certainly be of interest to repeat the generalised molecular field calculations to check the extent of this reduction. There are also other things that might be done. The most important of these would be to allow for the existence of other molecular conformations since the torsional energy differences for such dimers are comparable to thermal

energies. The resultant conformations, largely associated with the spacer chain, would necessarily have a range of molecular topologies. In addition the calculations would need to allow for the influence of the anisotropic environment of the nematic and twist-bend nematic phases on the conformational probability distribution [56].

To calculate the conformational distribution function and other properties for the liquid crystal dimers it is usual to employ an approach proposed by Marcelja [43] and widely used in other studies of nematics [57,58]. In addition to the conformational energies it is necessary to determine the anisotropic energy resulting from the interaction between the molecule and the director for each conformer at a given degree of order. Originally this evaluation was founded on a segmental approach [43], dividing the molecule into basic, rigid groups. More recently the anisotropic energy was defined in terms of the surface normal, the angle it made with the director and integrated over the surface for each conformer [58].

Such calculations provide a wealth of information about the conformations and so some thought needs to be given as to how this might best be interrogated. One option would be to calculate the angle between the two mesogenic groups often defined by their para-axes or long axes. This approach was used in the investigation of the dimer CB7CB [12,21] using continuous torsional potentials. What was found is that the largest conformational probability is for the interarm angle of about 115° in the isotropic and nematic phases. However the distribution centred on this angle is broad ranging over about 70° in the isotropic phase [21] and slightly less in the nematic phase [21]. In both phases there is a weak contribution to the distribution function from hair-pin conformers. It remains to be seen how the distribution of conformers about 115° can influence the formation of the N_{TB} phase given that the V-shaped model predicts the formation of the N_{TB} to occur when the interarm angle is about 135° .

An alternative strategy that has been explored is to use the conformational distribution to determine an average molecular shape of the dimers. The results shown for CB7CB were based on a simple model for the dimer with the methylene groups being represented by a single atom and the mesogenic groups by five atoms placed along the para-axis [60,61]. To average over the coordinates of the atoms it is necessary to define a common coordinate system in which the conformers can be placed. This is achieved by taking one conformer as a template, placing all other conformers on this and averaging their coordinates over all conformers. In addition to the average coordinates the deviation of atoms from their average positions is used to generate a set of fluctuational ellipsoids which are imposed on the average coordinates. This is analogous to the thermal ellipsoids employed to represent the molecular structures in X-ray crystallography. The average structure obtained in this way for the odd dimer model for CB7CB is certainly of interest with the truncated-V form clearly apparent; the atoms in the spacer form an essentially linear array with the mesogenic groups tilted with respect to it. This supports the potential value of studying the phase behaviour of such images with the aid of the generalised molecular field calculations [24].

Until such calculations are performed it might be difficult to see how the phase behaviour is to be viewed from the average structure of the odd dimers.

It should be apparent that for realistic models of liquid crystal dimers because their geometric properties result from the molecular flexibility are likely to be complex. This is unlike the single interarm angle of the V-shape model and that of the ground-state conformer. It seems we should seek, instead, a single property whose value is directly related to the $N_{TB} - N$ transition. One such property was identified by Dozov in his Landau-like theory of the N_{TB} phase [6]. Here it is the elastic constants of the nematic phase which play a dominant role with the N_{TB} phase appearing when the bend elastic constant, K_3 , vanishes; provided $K_1/2K_2 > 1$. To value the usefulness of this approach we first consider the calculation of the three elastic constants which includes the molecular flexibility and the complexity of the molecular structure as a function of the orientational order [62]. Results obtained for the non-symmetric dimers, α -(2',4-difluorobiphenyl-4'-yloxy)- ω -(4-cyanobiphenyl-4'-yloxy)alkanes, show that for the even dimers all three elastic constants increase with increasing orientational order, as expected, while for odd dimers both K_1 and K_2 also increase. In marked contrast K_3 decreases with increasing order. Such behaviour has been observed for a mixture of ether-linked dimers doped with a methylene-linked dimer [48] and for CB7CB [63] while for other systems K_3 does not approach so close to zero as the N_{TB} phase is approached [64]. More specifically, for the odd dimers, FFO5OCB and FFO7OCB, K_3 for the ether-linked pentane spacer passes to zero when the order parameter for the cyanobiphenyl group is about 0.42 while for the ether-linked heptane spacer it is about 0.50. This suggests that the transition to the N_{TB} phase occurs at a higher temperature for FFO5OCB than for FFO7OCB.

In this relatively brief discussion we have raised a number of issues concerning the molecular factors responsible for the twist-bend nematic phase. The problem is certainly made challenging by the molecular flexibility associated with the spacer linking the mesogenic groups and hence influencing the molecular curvature. This makes the determination of the value of a single factor related to this curvature particularly difficult if not impossible. It seems that the use of a single well-defined parameter readily calculated could be of real assistance in understanding the design of mesogens capable of forming the twist-bend nematic. We have suggested that one such property would be the bend elastic constant and that this might be evaluated from the generalised molecular field theory which would allow the molecular factors responsible for K_3 vanishing to be explored.

Appendix B: Transitional data for the *mO.n.Om* dimers

Here the transition temperatures, molar enthalpies and dimensionless entropies are listed for the dimers with spacer length, n , and terminal chain length m . Some of these dimers have been prepared previously and these are indicated by the reference [2].

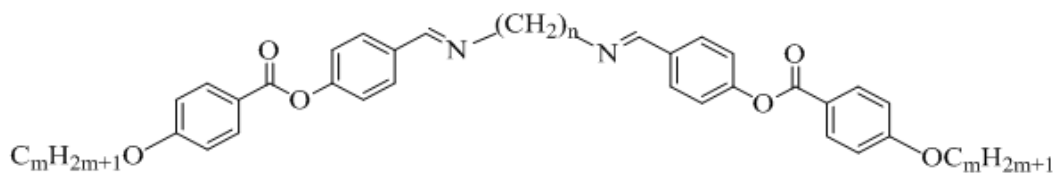


Table A1. Transition temperatures ($^{\circ}\text{C}$), enthalpies (kJ mole^{-1}) in italics and scaled entropy values $\Delta S/R$, in square brackets, for dimers $mO.3.Om$. Round brackets indicate monotropic transitions.

Dimer	Cr	B ₆	N _{TB}	N	Iso
10.3.O1	•	118.2 <i>36.4</i> [11.2]	•	(60.3) <i>1.8</i> [0.66]	•
20.3.O2	•	143.8 <i>82.3</i> [23.7]	•	(87.4) <i>2.2</i> [0.76]	•
30.3.O3	•	147.6 <i>51.1</i> [14.6]	•	(62) <i></i>	•
40.3.O4	•	115.9 <i>38.7</i> [12]	•	(105.2) <i>9.2</i> [2.9]	•
50.3.O5	•	122.2 <i>57.9</i> [17.6]	•	(108.3) <i>10.9</i> [3.4]	•

6O.3.O6	•	121	•	(115.1)	•
		58.2[17.8]		13.5[4.2]	

Table A2. Transition temperatures (°C), enthalpies (kJ mole⁻¹) in italics and scaled entropy values $\Delta S/R$, in square brackets, for dimers mO.5.Om. Round brackets indicate monotropic transitions.

Dimer	Cr	B ₆	N _{TB}	N	Iso
1O.5.O1	•	114.4	•	(79.1)	•
		<i>43.3</i> [13.4]		<i>0.29</i> [0.10]	<i>0.13</i> [0.04]
2O.5.O2	•	119.0	•	(93.9)	•
		<i>49.5</i> [15.2]		<i>0.40</i> [0.13]	<i>0.21</i> [0.06]
3O.5.O3	•	126			•
		<i>44.5</i> [13.4]			
4O.5.O4 [2]	•	118.9	•	(98.5)	•
		<i>59.3</i> [18.2]	<i>5.7</i> [1.8]		<i>0.23</i> [0.07]
5O.5.O5	•	105.6	•	109.1	•
		<i>37.2</i> [11.8]	<i>9.3</i> [2.9]		
6O.5.O6 [2]	•	124	•	(116.6)	•
		<i>60.5</i> [18.3]	<i>11.1</i> [3.4]		

Table A3. Transition temperatures (°C), enthalpies (kJ mole⁻¹) in italics and scaled entropy values $\Delta S/R$, in square brackets, for dimers mO.7.Om. Round brackets indicate monotropic transitions.

Dimer	Cr	B ₆	N _{TB}	N	Iso
1O.7.O1	•	127.8	•	(94.3)	•
		<i>44.4</i> [13.3]		<i>0.21</i> [0.07]	<i>0.45</i> [0.14]
2O.7.O2	•	95.2	•	104.3	•

		38.5[12.6]		0.39[0.12]	0.33[0.10]	
3O.7.O3	•	105.7		(83.3)	(101.8)	•
		50.6[16.1]		0.40[0.13]	0.25[0.08]	
4O.7.O4 [2]	•	109.5		(96.4)	112.1	•
		43.4[13.6]		0.60[0.20]	0.37[0.12]	
5O.7.O5	•	96.5	•	104.9		•
		29.8[9.7]		8.3[2.6]		
6O.7.O6 [2]	•	93.0	•	116.2		•
		43.2[14.2]		11.2[3.5]		

Table A4. Transition temperatures (°C), enthalpies (kJ mole⁻¹) in italics and scaled entropy values $\Delta S/R$, in square brackets, for dimers mO.9.Om. Round brackets indicate monotropic transitions.

Dimer	Cr	B6'	B ₆	N _{TB}	N	Iso
1O.9.O1	•	119.9		•	(92.4)	•
		53.3[16.3]			0.27[0.09]	0.45[0.14]
2O.9.O2	•	93.2		•	102.6	•
		43.9[14.4]			0.61[0.20]	1.57[0.46]
3O.9.O3	•	96.8		•	(87.6)	•
		39.5[12.8]			0.23[0.08]	0.58[0.18]
4O.9.O4	•	90.8		•	96.1	•
		32.9[10.9]			0.67[0.22]	0.55[0.17]
5O.9.O5	•	98.1	•	(94.7)	•	108.8
		51.6[16.7]		5.4[1.8]		0.65[0.21]
6O.9.O6	•	79.0	•	85.5	•	104.4
		26.1[8.9]		1.6[0.5]		10.2[3.3]

Table A5. Transition temperatures (°C), enthalpies (kJ mole⁻¹) in italics and scaled entropy values $\Delta S/R$, in square brackets, for dimers mO.11.Om. Round brackets indicate monotropic transitions.

Dimer	Cr	B ₆	N _{TB}	N	Iso
1O.11.O1	• 92.3 <i>46.5</i> [15.3]		• <i>94.6</i> • <i>0.07</i> [0.02]	123.7 • <i>1.05</i> [0.32]	
2O.11.O2	• 96.0 <i>48.3</i> [15.7]		• 104.2 • <i>0.03</i> [0.02]	• 133.3 <i>1.6</i> [0.46]	•
3O.11.O3	• 99.7 <i>45.4</i> [14.6]			• 110.5 0.84[0.26]	•
4O.11.O4	• 100.3 <i>55.2</i> [17.8]		• (92.6) <i>0.23</i> [0.08]	• 118.0 <i>0.93</i> [0.29]	•
5O.11.O5	• 89.1 <i>41.2</i> [13.7]	• (89.4) 3.9[1.3]		• 111.5 <i>1.02</i> [0.32]	•
6O.11.O6	• 94.5 <i>4.3</i> [1.4]	• 108.5 <i>6.6</i> [2.1]		• 114.8 <i>1.44</i> [0.45]	•

